ASME VIII Nozzle Local-Load Report

Method: WRC 537 with WRC 297

Cylinder — Circular Hollow Nozzle

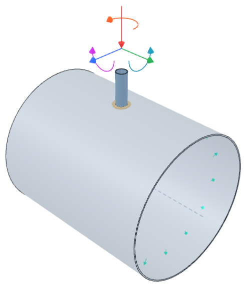

Nozzle Design 3D Model

Project Details

Project	Separator V-101
Project ID	PVC-SAMPLE-01
Company	PV Cloud
Client	Sample Project
Designer	PV Cloud
Units	metric
Design Code	ASME BPVC Section VIII, Div 1 & 2 (2023)
Vessel Type	Cylinder
Nozzle Type	Circular Hollow

August 19, 2026

Contents

Disclaimer

IMPORTANT DISCLAIMER

This calculation tool is provided for informational and preliminary design purposes only. All results must be independently verified and signed off by a qualified and competent engineer before use in any engineering design, submission, or fabrication process. The developers of this tool accept no responsibility or liability for the use of this output in any professional capacity.

By proceeding with the use of this document, you acknowledge and agree to these terms.

1. Scope and Method

This report presents an evaluation of local primary membrane, bending, and shear stresses at the nozzle–shell junction of a cylindrical pressure vessel with a circular hollow nozzle. The analysis considers the effects of internal pressure and external nozzle loadings in accordance with WRC 537 and supplemental guidance from WRC 297. Where applicable, pressure intensification effects and additional rules (e.g., pressure intensification per PVP Vol. 399) are incorporated.

Governing code: the calculated stresses are compared to the allowable limits of **ASME BPVC Section VIII, Divisions 1 and 2**.

Assumptions: The analysis assumes linear-elastic material behavior, small deformations, and a thin shell geometry within the valid parameter ranges of the referenced charts.

Weld joint efficiency: a joint efficiency of $\Phi = 1.0$ is assumed for all seams — the ASME VIII-1 UW-12 fully-radiographed equivalent — and the nozzle is assumed to be clear of the shell weld seams. No weld stress-concentration factor and no fatigue-strength-reduction factor is applied. Where a seam is not fully radiographed, or the opening falls on or near a seam, the demands in this report must be re-checked against the applicable UW-12 joint efficiency.

2. Warnings

No warnings.

3. Inputs

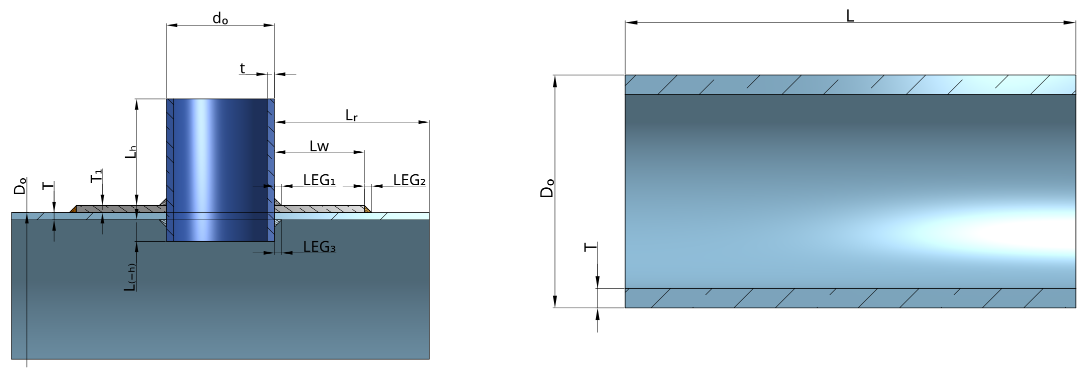

(a) **(b)**

Figure 3.1 Input geometry reference: (a) Nozzle; (b) Vessel

Table 3.1 Geometry

Description	Symbol	Value
Outer Vessel Diameter	D_o	3600 mm
Vessel Thickness	T	30 mm
Outer Nozzle Diameter	d_o	273.1 mm
Nozzle Thickness	t	15.09 mm
Fillet Radius	r_f	8 mm
Junction Type	—	Set-on with reinforcing pad
Reinforcement (BPVC UG-37, Bildy §5)		
Pad Outer Diameter	D_p	430 mm
Pad Thickness	s_2	14 mm
Pad Radial Width	l_2	78.45 mm
Base Weld Leg	Δ	10 mm
Nozzle Weld Leg	Δ_1	10 mm
Pad Weld Leg	Δ_2	8 mm

Corrosion allowance applied:
Shell: $c_{shell} = 3.50$ mm (C1 = 3.00 + C2 = 0.50 + C3 = 0.00)
Nozzle: $c_{nozzle} = 1.50$ mm (C1 = 1.50 + C2 = 0.00 + C3 = 0.00)
Effective shell wall: $T_{eff} = T - c_{shell} = 30.00 - 3.50 = 26.50$ mm
Effective nozzle wall: $t_{eff} = t - c_{nozzle} = 15.09 - 1.50 = 13.59$ mm

Table 3.2 Vessel Materials

Item	Symbol	Value
Shell material		SA-516-70-plate
Yield strength (design)	S_y	255.6 MPa (50 °C)
Yield strength (cold)	$S_{y,\text{cold}}$	262 MPa (21 °C)
Yield strength (room temp.)	$S_{y,\text{RT}}$	260 MPa
Tensile strength	UTS	485 MPa
Allowable (Div 1)	S	138 MPa
Allowable (cold, Div 1)	S_{cold}	138 MPa
Allowable (Div 2)	S	170.6 MPa
Allowable (cold, Div 2)	S_{cold}	175 MPa

Material data is from ASME BPVC 2021 Section II, Part D (metric).

Table 3.3 Nozzle Materials

Item	Symbol	Value
Nozzle material		SA-106-B-pipe
Yield strength (design)	S_y	235.4 MPa (50 °C)
Yield strength (cold)	$S_{y,\text{cold}}$	241 MPa (21 °C)
Yield strength (room temp.)	$S_{y,\text{RT}}$	240 MPa
Tensile strength	UTS	415 MPa
Allowable (Div 1)	S	118 MPa
Allowable (cold, Div 1)	S_{cold}	118 MPa
Allowable (Div 2)	S	157 MPa
Allowable (cold, Div 2)	S_{cold}	161 MPa

Material data is from ASME BPVC 2021 Section II, Part D (metric).

Table 3.4 Design Loads

Load	Symbol	Value
Pressure	p	1.2 MPa
Working Condition	—	Operating / Design
Radial load	F	5 kN
Shear (circumferential)	V_C	1.2 kN
Shear (longitudinal)	V_L	1.5 kN
Moment (circumferential)	M_C	0.8 kN m
Moment (longitudinal)	M_L	0.8 kN m
Torsion	M_T	0.6 kN m

Design Loads by Load Case

Table 3.5 Applied loads per load case, as entered

LC	Working Condition	p (MPa)	F_R (kN)	V_C (kN)	V_L (kN)	M_C (kN m)	M_L (kN m)	M_T (kN m)
1	Operating / Design	1.2	5	1.2	1.5	0.8	0.8	0.6
2	Test (general)	1.56	2.5	0.6	0.75	0.4	0.4	0.3

p is the effective pressure each load case was evaluated at (design pressure plus any hydrostatic head). The resulting demands and acceptance verdict per load case are in the Per-Load-Case Results section.

4. Allowable Limits

S_{PL} and S_{PS} are single limits for the assembly. They are evaluated on the *governing* properties — the lesser of the vessel and nozzle values, written S^g, S^g_{cold}, S^g_y, $S^g_{y,\mathrm{cold}}$ — and the same two limits then apply to both components. $S^g_y = 235.4\,\mathrm{MPa}$, $S^g_{y,\mathrm{cold}} = 241\,\mathrm{MPa}$.
Both limits carry a ductility guard. ASME VIII-2 §5.2.2.4, Step 5(b) (p. 583) and §5.5.6.1(d)(2) (p. 598) direct that the S_y term *is not used* — leaving $1.5S$ and $3S$ respectively — when the ratio of specified minimum yield strength to ultimate tensile strength exceeds 0.70, or when S is governed by time-dependent (creep) properties. Where the guard is active the equation below shows only the term that survives, and says so.

4.1 Vessel allowable limits

Material: SA-516-70-plate (50 °C)

Allowable stress equations adopted for the vessel are shown below for both Division 1 and Division 2 (per **ASME BPVC.VIII.1&2 (2023)**). Symbols are the same as for the nozzle. Unless otherwise noted, the safety factor is taken as $F_s = 1$.

Division 1

$$S_{\mathrm{Div1}} = \frac{S_{\mathrm{tab}}}{F_s} = \frac{138}{1} = 138\,MPa \qquad S^g_{\mathrm{Div1}} = 118\,MPa \tag{4.1}$$

$$S_{PL,\,\mathrm{Div1}} = \max\left\{1.5\,S^g_{\mathrm{Div1}},\ S^g_y\right\} = \max\left\{1.5 \times 118,\ 235.4\right\} = 235.4\,MPa \tag{4.2}$$

$$\begin{aligned} S_{PS,\,\mathrm{Div1}} &= \max\left\{1.5\left(S^g_{\mathrm{cold,\,Div1}} + S^g_{\mathrm{Div1}}\right),\ S^g_{y,\mathrm{cold}} + S^g_y\right\} \\ &= \max\left\{1.5\,(118 + 118)\,,\ 241 + 235.4\right\} = 476.4\,MPa \end{aligned} \tag{4.3}$$

Division 2

$$S_{\mathrm{Div2}} = \frac{S_{\mathrm{tab}}}{F_s} = \frac{170.6}{1} = 170.6\,MPa \qquad S^g_{\mathrm{Div2}} = 157\,MPa \tag{4.4}$$

$$S_{PL,\,\mathrm{Div2}} = \max\left\{1.5\,S^g_{\mathrm{Div2}},\ S^g_y\right\} = \max\left\{1.5 \times 157,\ 235.4\right\} = 235.5\,MPa \tag{4.5}$$

$$\begin{aligned} S_{PS,\,\mathrm{Div2}} &= \max\left\{1.5\left(S^g_{\mathrm{cold,\,Div2}} + S^g_{\mathrm{Div2}}\right),\ S^g_{y,\mathrm{cold}} + S^g_y\right\} \\ &= \max\left\{1.5\,(161 + 157)\,,\ 241 + 235.4\right\} = 477\,MPa \end{aligned} \tag{4.6}$$

4.2 Nozzle allowable limits

Material: SA-106-B-pipe (50 °C)

Allowable stress equations adopted for the nozzle are shown below. They are presented for both Division 1 and Division 2 (per **ASME BPVC.VIII.1&2 (2023)**). Symbols: S (allowable at temperature), S_{cold} (allowable at ambient), S_y (yield); a superscript g marks a governing value. Unless otherwise noted, the safety factor is taken as $F_s = 1$.

Division 1

$$S_{\text{Div1}} = \frac{S_{\text{tab}}}{F_s} = \frac{118}{1} = 118\,MPa \qquad S^g_{\text{Div1}} = 118\,MPa \tag{4.7}$$

$$S_{PL,\,\text{Div1}} = \max\left\{1.5\,S^g_{\text{Div1}},\ S^g_y\right\} = \max\left\{1.5 \times 118,\ 235.4\right\} = 235.4\,MPa \tag{4.8}$$

$$\begin{aligned} S_{PS,\,\text{Div1}} &= \max\left\{1.5\left(S^g_{\text{cold,\,Div1}} + S^g_{\text{Div1}}\right),\ S^g_{y,\text{cold}} + S^g_y\right\} \\ &= \max\left\{1.5\left(118 + 118\right),\ 241 + 235.4\right\} = 476.4\,MPa \end{aligned} \tag{4.9}$$

Division 2

$$S_{\text{Div2}} = \frac{S_{\text{tab}}}{F_s} = \frac{157}{1} = 157\,MPa \qquad S^g_{\text{Div2}} = 157\,MPa \tag{4.10}$$

$$S_{PL,\,\text{Div2}} = \max\left\{1.5\,S^g_{\text{Div2}},\ S^g_y\right\} = \max\left\{1.5 \times 157,\ 235.4\right\} = 235.5\,MPa \tag{4.11}$$

$$\begin{aligned} S_{PS,\,\text{Div2}} &= \max\left\{1.5\left(S^g_{\text{cold,\,Div2}} + S^g_{\text{Div2}}\right),\ S^g_{y,\text{cold}} + S^g_y\right\} \\ &= \max\left\{1.5\left(161 + 157\right),\ 241 + 235.4\right\} = 477\,MPa \end{aligned} \tag{4.12}$$

Division 2 allowable class: the S_{tab} values used above for Division 2 are taken from **ASME BPVC Section II-D, Tables 5A/5B**, which tabulate allowable stresses for **Section VIII, Division 2, Class 2** construction (II-D, paras. 2.7 and 2.8, p. 4). Division 2, Class 1 allowables — II-D Tables 2A/2B, paras. 2.3 and 2.4 — are not included in this tool, so every Division 2 result in this report is a Class 2 assessment. Division 1 values are from II-D Tables 1A/1B.

4.3 Pad weld-toe acceptance check

Reference: BPVC UG-37 area-replacement, Bildy §5.4 pad-edge membrane stress.

$\sigma_{\text{pad\_edge}}$ vs S_{PL}: 97.5 MPa against a limit of 235.4 MPa

No verdict: the calculation reports the pad weld-toe stress but issues no acceptance verdict for this point, so none is stated here. The demand and the limit are printed so the comparison can be made and recorded by the engineer.

5. Results

Point key. Stresses are reported at the eight standard WRC junction points. A and B are the two points where the attachment meets the shell's longitudinal plane of symmetry, C and D the two points on the transverse plane (WRC 537 Figure 1; WRC 297 §3.4). The subscript is the shell surface: u = upper (outer) surface, L = lower (inner) surface — so A_u is the outer surface at point A and C_L the inner surface at point C. Membrane stresses are equal at u and L; bending stresses change sign through the wall.

5.1 Nozzle results

Table 5.1 Nozzle stresses summary

Circumferential stresses, σ_θ	A_u	A_L	B_u	B_L	C_u	C_L	D_u	D_L
Membrane due to F (Eq. C.10)	-0.4899	-0.4899	-0.4899	-0.4899	-0.4899	-0.4899	-0.4899	-0.4899
Membrane due to M_c (Eq. C.11)					-0.0251	-0.0251	0.0251	0.0251
Membrane due to M_L (Eq. C.12)	-0.2635	-0.2635	0.2635	0.2635				
Circumferential stress due to pressure $\sigma_{\theta,p}$ (Eq. C.13 & Eq. C.14)	158.91	158.91	158.91	158.91	81.032	81.032	81.032	81.032
Circumferential membrane stress due to pressure $P_{\theta,m}$ (Eq. C.15)	92.82	92.82	92.82	92.82	46.41	46.41	46.41	46.41
Total circumferential membrane stress $\sigma_{\theta,m}$ (Eq. C.16 & Eq. C.17)	158.15	158.15	158.68	158.68	80.517	80.517	80.567	80.567
Total circumferential stresses σ_θ (Eq. C.18 & Eq. C.19)	158.15	158.15	158.68	158.68	80.517	80.517	80.567	80.567
Longitudinal stresses, σ_r	A_u	A_L	B_u	B_L	C_u	C_L	D_u	D_L
Membrane due to F (Eq. C.20)	-0.2044	-0.2044	-0.2044	-0.2044	-0.2044	-0.2044	-0.2044	-0.2044
Bending due to F (Eq. C.22)	-5.5648	5.5648	-5.5648	5.5648	-5.5648	5.5648	-5.5648	5.5648
Membrane due to M_c (Eq. C.23)					-0.5348	-0.5348	0.5348	0.5348
Bending due to M_c (Eq. C.25)					-5.4862	5.4862	5.4862	-5.4862
Membrane due to M_L (Eq. C.26)	-0.5348	-0.5348	0.5348	0.5348				
Bending due to M_L (Eq. C.28)	-4.3675	4.3675	4.3675	-4.3675				
Longitudinal stress due to pressure $\sigma_{r,p}$ (Eq. C.29)	5.9111	5.9111	5.9111	5.9111	5.9111	5.9111	5.9111	5.9111
Longitudinal membrane stress due to pressure $P_{r,m}$ (Eq. C.30)	5.9111	5.9111	5.9111	5.9111	5.9111	5.9111	5.9111	5.9111
Total longitudinal membrane stress $\sigma_{r,m}$ (Eq. C.31 & Eq. C.32)	5.1718	5.1718	6.2415	6.2415	5.1718	5.1718	6.2415	6.2415
Total longitudinal stresses σ_r (Eq. C.33 & Eq. C.34)	-4.7604	15.104	5.0442	7.4388	-5.8792	16.223	6.1629	6.3201
Shear stresses, τ	A_u	A_L	B_u	B_L	C_u	C_L	D_u	D_L
Shear stresses due to M_t (Eq. C.35)	0.1697	0.1697	0.1697	0.1697	0.1697	0.1697	0.1697	0.1697
Shear stresses due to F_C (Eq. C.36)	0.0927	0.0927	-0.0927	-0.0927				
Shear stresses due to F_L (Eq. C.37)					-0.1159	-0.1159	0.1159	0.1159
Total shear stresses τ (Eq. C.38 & Eq. C.39)	0.2624	0.2624	0.077	0.077	0.0538	0.0538	0.2856	0.2856
Total stresses	A_u	A_L	B_u	B_L	C_u	C_L	D_u	D_L
Membrane stress due to pressure P_m (Eq. C.30)	92.82	92.82	92.82	92.82	46.41	46.41	46.41	46.41
Membrane stress σ_m (Eq. C.40)	158.15	158.15	158.68	158.68	80.517	80.517	80.568	80.568
Total stress σ (Eq. C.41)	162.92	162.92	158.68	158.68	86.396	86.396	80.568	80.568

Acceptance summary (ASME BPVC.VIII.1&2 (2023))

The demand and limit on each line are shown for reference; the acceptance verdict below each division is the calc engine's, and it covers the junction as a whole.

Division 1

$P_m \leq S$: 92.8 MPa ≤ 118 MPa

$\sigma_{m,\mathrm{eqv}} \leq S_{PL}$: 158.7 MPa ≤ 235.4 MPa

$\sigma_{\mathrm{eqv}} \leq S_{PS}$: 162.9 MPa ≤ 476.4 MPa

Division 1 verdict: PASS

Division 2

$P_m \leq S$: 92.8 MPa ≤ 157 MPa

$\sigma_{m,\mathrm{eqv}} \leq S_{PL}$: 158.7 MPa ≤ 235.5 MPa

$\sigma_{\mathrm{eqv}} \leq S_{PS}$: 162.9 MPa ≤ 477 MPa

Division 2 verdict: PASS

5.2 Vessel results

Table 5.2 Vessel stresses summary

Circumferential stresses, σ_θ	A_u	A_L	B_u	B_L	C_u	C_L	D_u	D_L
Membrane due to F (Eq. C.52 & Eq. C.53)	-0.5171	-0.5171	-0.5171	-0.5171	-0.4887	-0.4887	-0.4887	-0.4887
Bending due to F (Eq. C.54 & Eq. C.55)	-1.783	1.783	-1.783	1.783	-2.4199	2.4199	-2.4199	2.4199
Membrane due to M_c (Eq. C.56)					-0.095	-0.095	0.095	0.095
Bending due to M_c (circumferential) (Eq. C.57)					-2.2612	2.2612	2.2612	-2.2612
Membrane due to M_L (Eq. C.58)	-0.3552	-0.3552	0.3552	0.3552				
Bending due to M_L (circumferential) (Eq. C.59)	-1.1506	1.1506	1.1506	-1.1506				
Circumferential stress due to pressure $\sigma_{\theta,p}$ (Eq. C.60 & Eq. C.61)	158.91	158.91	158.91	158.91	92.82	92.82	92.82	92.82
Circumferential membrane stress due to pressure $P_{\theta,m}$ (Eq. C.62)	92.82	92.82	92.82	92.82	92.82	92.82	92.82	92.82
Total circumferential membrane stress $\sigma_{\theta,m}$ (Eq. C.63 & Eq. C.64)	158.04	158.04	158.75	158.75	92.236	92.236	92.426	92.426
Total circumferential stresses σ_θ (Eq. C.65 & Eq. C.66)	155.1	160.97	158.11	159.38	87.555	96.917	92.268	92.585
Longitudinal stresses, σ_r	A_u	A_L	B_u	B_L	C_u	C_L	D_u	D_L
Membrane due to F (Eq. C.67 & Eq. C.68)	-0.4887	-0.4887	-0.4887	-0.4887	-0.5171	-0.5171	-0.5171	-0.5171
Bending due to F (Eq. C.69 & Eq. C.70)	-2.4338	2.4338	-2.4338	2.4338	-1.7693	1.7693	-1.7693	1.7693
Membrane due to M_C (Eq. C.71)					-0.1338	-0.1338	0.1338	0.1338
Bending due to M_C (Eq. C.72)					-1.267	1.267	1.267	-1.267
Membrane due to M_L (Eq. C.73)	-0.0956	-0.0956	0.0956	0.0956				
Bending due to M_L (Eq. C.74)	-1.8383	1.8383	1.8383	-1.8383				
Longitudinal stress due to pressure $\sigma_{r,p}$ (Eq. C.76 & Eq. C.75)	46.41	46.41	46.41	46.41	81.032	81.032	81.032	81.032
Longitudinal membrane stress due to pressure $P_{r,m}$ (Eq. C.77)	46.41	46.41	46.41	46.41	46.41	46.41	46.41	46.41
Total longitudinal membrane stress $\sigma_{r,m}$ (Eq. C.78 & Eq. C.79)	45.826	45.826	46.017	46.017	80.381	80.381	80.649	80.649
Total longitudinal stresses σ_r (Eq. C.80 & Eq. C.81)	41.554	50.098	45.421	46.613	77.345	83.417	80.146	81.151
Shear stresses, τ	A_u	A_L	B_u	B_L	C_u	C_L	D_u	D_L
Shear stresses due to M_t (Eq. C.82)	0.0854	0.0854	0.0854	0.0854	0.0854	0.0854	0.0854	0.0854
Shear stresses due to F_C (Eq. C.83)	0.0466	0.0466	-0.0466	-0.0466				
Shear stresses due to F_L (Eq. C.84)					-0.0583	-0.0583	0.0583	0.0583
Total shear stresses τ (Eq. C.85 & Eq. C.86)	0.132	0.132	0.0387	0.0387	0.0271	0.0271	0.1436	0.1436
Total stresses	A_u	A_L	B_u	B_L	C_u	C_L	D_u	D_L
Membrane stress due to pressure P_m (Eq. C.62)	92.82	92.82	92.82	92.82	92.82	92.82	92.82	92.82
Membrane stress σ_m (Eq. C.87)	158.04	158.04	158.75	158.75	92.236	92.236	92.428	92.428
Total stress σ (Eq. C.88)	160.97	160.97	159.38	159.38	96.917	96.917	92.587	92.587

Pad weld-toe stress (Bildy §5.4 / location: pad_edge)

Table 5.3 Reinforcing pad — edge (weld-toe) membrane stress

Quantity	Value
Effective pad wall $T + s_2 + s_3 - c$	30 mm
Junction factor κ	1.05
Membrane hoop $\sigma_{\theta,m}$ at pad edge	97.461 MPa
Membrane longitudinal $\sigma_{x,m}$ at pad edge	48.759 MPa
Stress intensity S at pad edge	97.461 MPa

Acceptance summary (ASME BPVC.VIII.1&2 (2023))

The demand and limit on each line are shown for reference; the acceptance verdict below each division is the calc engine's, and it covers the junction as a whole.

Division 1
$P_m \leq S$: 92.8 MPa ≤ 118 MPa
$\sigma_{m,\text{eqv}} \leq S_{PL}$: 158.7 MPa ≤ 235.4 MPa
$\sigma_{\text{eqv}} \leq S_{PS}$: 161 MPa ≤ 476.4 MPa
Division 1 verdict: PASS

Division 2
$P_m \leq S$: 92.8 MPa ≤ 157 MPa
$\sigma_{m,\text{eqv}} \leq S_{PL}$: 158.7 MPa ≤ 235.5 MPa
$\sigma_{\text{eqv}} \leq S_{PS}$: 161 MPa ≤ 477 MPa
Division 2 verdict: PASS

Per-Load-Case Results

Each row is the demand for one load case evaluated independently; the headline ASME acceptance above reflects the governing (worst-case) load case. Demands and allowables are in MPa.

Table 5.4 Per-load-case acceptance summary

LC	WorkCond	p (MPa)	T_v (°C)	T_n (°C)	P_m	$P_L + P_b$	$P_L + P_b + Q$	All
1	Operating / Design	1.20	50	50	78.31^{P}	146.20^{P}	166.50^{P}	477.00 (
2	Test (general)	1.56	50	50	90.01^{P}	158.75^{P}	162.92$^{n/e}$	216.90 (0.9

The Result column is the calc engine's verdict for the load case — every category that applies to it, per ASME VIII-2 §5.2.2.2 Step 5 — and the superscript on each demand is that category's own verdict: ^{P} accepted, ^{F} rejected, $^{n/e}$ no verdict issued. A test load case carries $^{n/e}$ on $P_L + P_b + Q$ because ASME VIII-2 §5.2.2.5 does not evaluate the secondary range in the test condition; the Allowable column still shows the test limit, which governs the primary categories only.
Allowable per ASME VIII-1 UG-99 / UG-100 and VIII-2 Part 4.4: $1.5\,S$ for design / operating, $0.9\,S_y$ for hydrotest (UG-99(b)) and generic test, $0.8\,S_y$ for pneumatic test (UG-100).

WRC 297 Validity Assessment

Per WRC Bulletin 297 §3.2 (Steele shallow-shell limits) and §3.3 (shear-stress accuracy caveat). PVCloud verifies the five thin-shell ratios computed from the input geometry; the four boundary-condition attestations (no internal protrusion, $\geq 2\sqrt{DT}$ / $\geq 2\sqrt{dt}$ clearance, through-penetration weld, $\geq 2\sqrt{dt}$ axial length when the nozzle thickness differs from the branch pipe) are user attestations and are NOT verified by PVCloud.

Table 5.5 WRC 297 §3.2 / §3.3 validity-band assessment

Variable	Actual	Min	Max	Status	Reference
d/D	0.076	—	0.5	OK	WRC 297 §3.2 (shallow-shell limit)

Variable	Actual	Min	Max	Status	Reference
d/t	20.1	20	—	OK	WRC 297 §3.2 (Steele thin-shell)
d/t	20.1	—	100	OK	WRC 297 §3.2 (Figs 3-58 d/t ≤ 100 limit)
D/T	134.85	20	—	OK	WRC 297 §3.2 (Steele thin-shell)
d/T	10.31	5	—	OK	WRC 297 §3.2 (Steele thin-shell)
D/T	134.85	—	2500	OK	WRC 297 §3.2 (recommended D/T upper limit)
$d/D(shear)$	0.076	0	0.1	OK	WRC 297 §3.3

Source: WRC Bulletin 297 §3.2 (Steele shallow-shell limits, p. 4) and §3.3 (shear-stress accuracy caveat).

6. Conclusion

Design Conclusion — worst cases

Nozzle worst-case total stress intensity: **162.9 MPa**
Vessel worst-case total stress intensity: **161 MPa**

Governing check per component/division (smallest FoS, computed in this report)

Nozzle, Div. 1: $P_m \leq S$ — FoS = 1.2713

Nozzle, Div. 2: $\sigma_{m,\mathrm{eqv}} \leq S_{PL}$ — FoS = 1.4841

Vessel, Div. 1: $P_m \leq S$ — FoS = 1.2713

Vessel, Div. 2: $\sigma_{m,\mathrm{eqv}} \leq S_{PL}$ — FoS = 1.4835

Global worst case: Nozzle, Div. 1 — FoS = **1.2713**

Acceptance verdict (calc engine)

Division 1: ____ PASS
Division 2: ____ PASS

Design Recommendation: The design meets all stress requirements and is acceptable for the specified loads and conditions.

References

1. ASME Boiler and Pressure Vessel Code. Rules for Construction of Pressure Vessels. Section VIII, Divisions 1 and 2. 2023. **Governing design code for this report.**

2. WRC-537 (3rd Ed.). Precision Equations and Enhanced Diagrams for Local Stresses in Spherical and Cylindrical Shells Due to External Loadings for Implementation of WRC Bulletin 107. Welding Research Council Bulletin. 2022. The local-load coefficients in this report are read from WRC-537.

3. WRC-107. Local Stresses in Spherical and Cylindrical Shells due to External Loadings. Welding Research Council Bulletin. 1979. Cited for method lineage only — WRC-537 supersedes it and no coefficient in this report is taken from WRC-107.

4. WRC-297. Local Stresses in Cylindrical Shells due to External Loadings on Nozzles – Supplement to WRC Bulletin No. 107/537. Welding Research Council Bulletin. 1987.

5. Bildy, L. M. A Proposed Method for Finding Stress and Allowable Pressure in Cylinders with Radial Nozzles. ASME PVP Vol. 399, Pressure Vessel and Piping Codes and Standards; Codeware. Source of the pressure-intensification factors $I_{\theta,p}$ and $I_{r,p}$.

6. ASME Boiler and Pressure Vessel Code, Section II, Part D. 2021.

7. Bednar, H. H. Pressure Vessel Design Handbook, 2nd Edition. Source of the off-radial rule that hillside-nozzle loads are decomposed vectorially into the main vessel planes (Ch. 7 §7.5 item 4) and of the nozzle stiffness / thermal-discontinuity coefficients.

8. ASME Boiler and Pressure Vessel Code, Section VIII, Division 2. §4.5.6 defines the hillside nozzle on a cylinder through the chord offset D_X; Annex 5-D.2.1 gives the hillside pressure stress index, acknowledged in the method notes but not applied to the numbers.

A. Derived Parameters

This section captures quantities derived from the input geometry, materials, and loads used later in coefficient evaluations and example calculations.

$$D_i = D_o - 2T \tag{A.1}$$

$$D_m = D_i + T = D_o - T \tag{A.2}$$

$$d_i = d_o - 2t \tag{A.3}$$

$$d_m = d_i + t = d_o - t \tag{A.4}$$

WRC 537 non-dimensional geometrical parameters for coefficient evaluation

$$R_m = \frac{D_i + T}{2} \tag{A.5}$$

$$\gamma = \frac{R_m}{T} \tag{A.6}$$

$$\beta = 0.875\,\frac{r_0}{R_m} \tag{A.7}$$

WRC 297 non-dimensional geometrical parameters for coefficient calculations

$$\lambda = \frac{d_o}{D_m\sqrt{\frac{D_m}{T}}} \tag{A.8}$$

$$\eta = \frac{d_o}{t} \tag{A.9}$$

$$\rho = \frac{T}{t} \tag{A.10}$$

In λ, η and ρ the wall thicknesses T and t, and the nozzle diameter d_o, are the CORRODED values — the geometry above less the corrosion allowances — and each ratio is rounded to three decimals before the charts are read. The ratios actually used are stated with the WRC 297 chart reads.

B. Coefficient Extraction

B.1 Coefficient Extraction from WRC 297 Charts

B.1.1 Interpolation Rules

The WRC 297 influence coefficient charts are evaluated in two stages: first across T/t within a fixed figure at an exact d/t, then across figures by d/t if required. Specifically:

1. **Within a figure (varying T/t at fixed d/t):** interpolate linearly in T/t. With $t = (T/t)$,

$$Y(t, d) = y_1 + (y_2 - y_1)\,\frac{t - t_1}{t_2 - t_1} \tag{B.1}$$

   If $t = t_1 = t_2$, use the exact value $Y(t, d) = y_1$. WRC 297 §3.1 requires interpolation between the T/t lines but does not prescribe a rule, so both a linear and a logarithmic blend are admissible readings. Appendix A settles it empirically: reading the Example 1 case ($\lambda = 0.87$, $d/t = 80$, $T/t = 2.67$) against the Bulletin's own published Table A-1 values gives a mean absolute error of 4.5% under the linear blend against 8.1% under a logarithmic one.

2. **Across figures (varying d/t):** evaluate the result at the bracketing figure d/t boundaries and interpolate linearly in d/t:

$$y(d/t) = y(d/t)_{\text{lower}} + \frac{(d/t) - (d/t)_{\text{lower}}}{(d/t)_{\text{upper}} - (d/t)_{\text{lower}}}\left[y(d/t)_{\text{upper}} - y(d/t)_{\text{lower}}\right] \tag{B.2}$$

Extrapolation Neither WRC 297 nor WRC 537 sanctions extrapolation beyond the plotted line ranges. PVCloud therefore treats a read past the end of a curve in three ways. Inside the plotted range, the value is read and reported plainly. Past the plotted end but still inside the bound over which the stored curve fit remains a faithful continuation of the published line, a value exists: PVCloud reports it marked † — disclosing the extrapolation rather than withholding a number the engineer would otherwise have to guess at — and every stress computed from it carries the same mark. Past that bound no defensible value exists, and PVCloud refuses the read: the entry prints as – and the stresses that depend on it are reported as gaps, never as zeros. A daggered value is outside the Bulletin's published basis and should be confirmed by finite-element analysis before sign-off.

B.1.2 Worked Chart Read

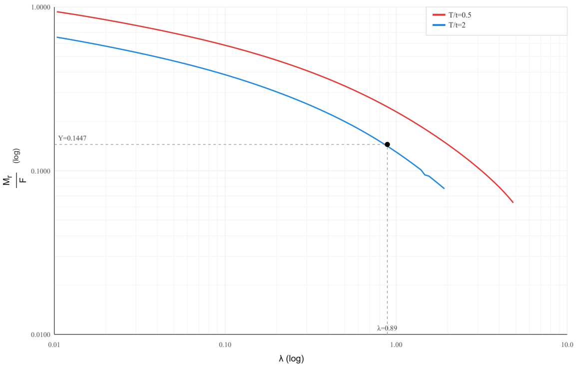

(a) (b)

Figure B.1 WRC 297 chart read for $\frac{M_r}{F}$ (a) $d/t =$ 20.0000 (b) $d/t =$ 30.0000

At $T/t = 1.9500$, $d/t = 20.0960$ and $\lambda = 0.8870$, $\frac{M_r}{F}$ is read on the two bracketing figures plotted above: Figure 4 at $d/t = 20.0000$ gives 0.1447 (Figure B.1(a)), and Figure 5 at $d/t = 30.0000$ gives 0.1510 (Figure B.1(b)), each after the T/t interpolation of Equation (B.1). Interpolating linearly across d/t per Equation (B.2) at $w = 0.0096$ gives $\frac{M_r}{F} = 0.1448$, reported in Table B.1.

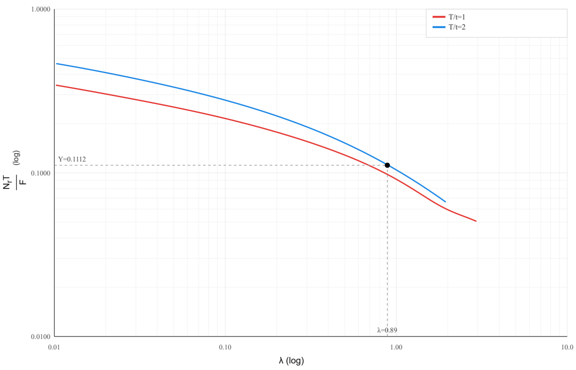

(a) (b)

Figure B.2 WRC 297 chart read for $\frac{N_r T}{F}$ (a) $d/t =$ 20.0000 (b) $d/t =$ 30.0000

At $T/t = 1.9500$, $d/t = 20.0960$ and $\lambda = 0.8870$, $\frac{N_r T}{F}$ is read on the two bracketing figures plotted above: Figure 9 at $d/t = 20.0000$ gives 0.1112 (Figure B.2(a)), and Figure 10 at $d/t = 30.0000$ gives 0.0961 (Figure B.2(b)), each after the T/t interpolation of Equation (B.1). Interpolating linearly across d/t per Equation (B.2) at $w = 0.0096$ gives $\frac{N_r T}{F} = 0.1111$, reported in Table B.1.

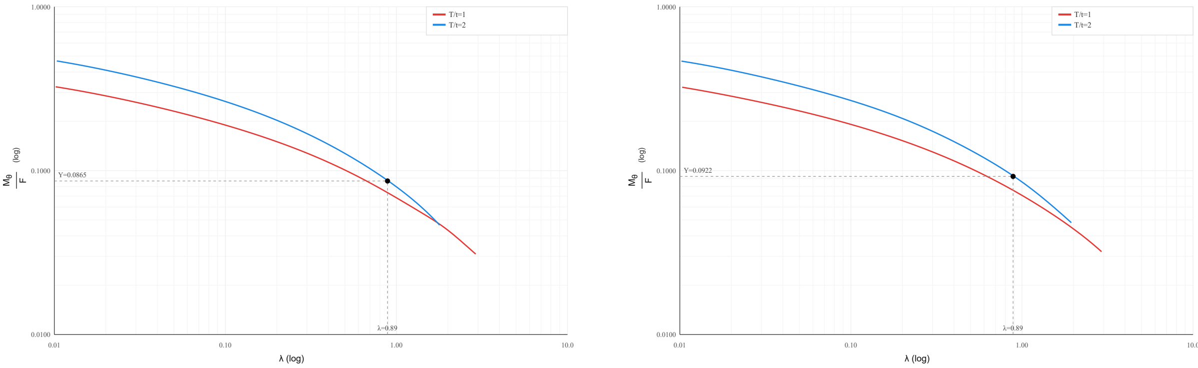

(a) **(b)**

Figure B.3 WRC 297 chart read for $\frac{M_\theta}{F}$ (a) $d/t =$ 20.0000 (b) $d/t =$ 30.0000

At $T/t = 1.9500$, $d/t = 20.0960$ and $\lambda = 0.8870$, $\frac{M_\theta}{F}$ is read on the two bracketing figures plotted above: Figure 14 at $d/t = 20.0000$ gives 0.0865 (Figure B.3(a)), and Figure 15 at $d/t = 30.0000$ gives 0.0922 (Figure B.3(b)), each after the T/t interpolation of Equation (B.1). Interpolating linearly across d/t per Equation (B.2) at $w = 0.0096$ gives $\frac{M_\theta}{F} = 0.0866$, reported in Table B.1.

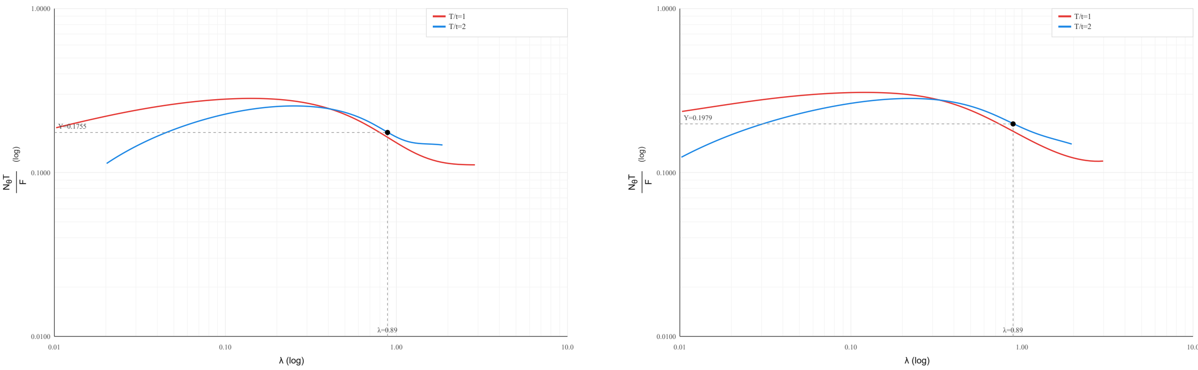

(a) **(b)**

Figure B.4 WRC 297 chart read for $\frac{N_\theta T}{F}$ (a) $d/t =$ 20.0000 (b) $d/t =$ 30.0000

At $T/t = 1.9500$, $d/t = 20.0960$ and $\lambda = 0.8870$, $\frac{N_\theta T}{F}$ is read on the two bracketing figures plotted above: Figure 19 at $d/t = 20.0000$ gives 0.1755 (Figure B.4(a)), and Figure 20 at $d/t = 30.0000$ gives 0.1979 (Figure B.4(b)), each after the T/t interpolation of Equation (B.1). Interpolating linearly across d/t per Equation (B.2) at $w = 0.0096$ gives $\frac{N_\theta T}{F} = 0.1758$, reported in Table B.1.

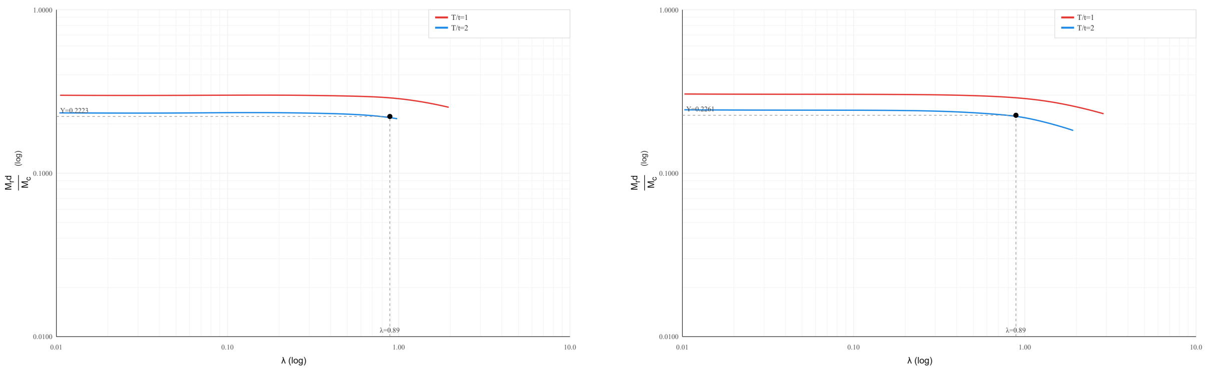

(a) **(b)**

Figure B.5 WRC 297 chart read for $\frac{M_r d}{M_c}$ (a) $d/t =$ 10.0000 (b) $d/t =$ 30.0000

At $T/t = 1.9500$, $d/t = 20.0960$ and $\lambda = 0.8870$, $\frac{M_r d}{M_c}$ is read on the two bracketing figures plotted above: Figure 23 at $d/t = 10.0000$ gives 0.2223 (Figure B.5(a)), and Figure 24 at $d/t = 30.0000$ gives 0.2261 (Figure B.5(b)), each after the T/t interpolation of Equation (B.1). Interpolating linearly across d/t per Equation (B.2) at $w = 0.5048$ gives $\frac{M_r d}{M_c} = 0.2242$, reported in Table B.1.

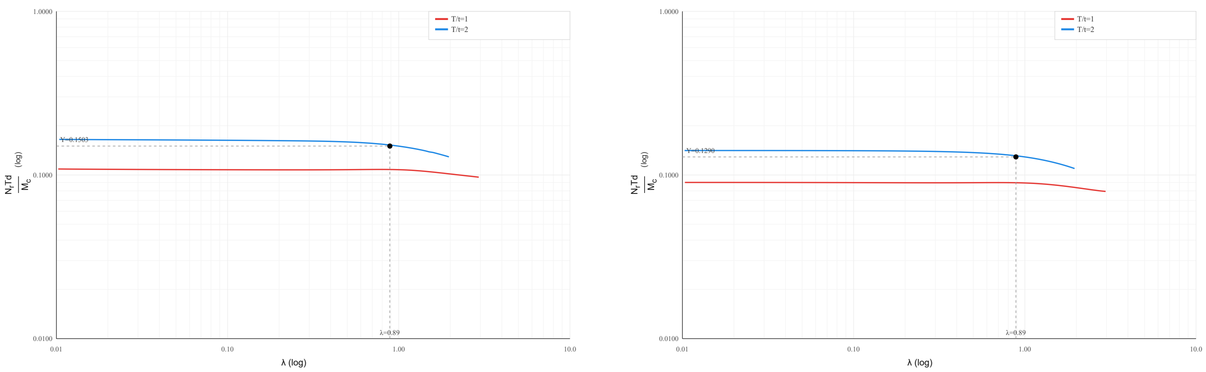

(a) **(b)**

Figure B.6 WRC 297 chart read for $\frac{N_r T d}{M_c}$ (a) $d/t =$ 20.0000 (b) $d/t =$ 30.0000

At $T/t = 1.9500$, $d/t = 20.0960$ and $\lambda = 0.8870$, $\frac{N_r T d}{M_c}$ is read on the two bracketing figures plotted above: Figure 28 at $d/t = 20.0000$ gives 0.1503 (Figure B.6(a)), and Figure 29 at $d/t = 30.0000$ gives 0.1290 (Figure B.6(b)), each after the T/t interpolation of Equation (B.1). Interpolating linearly across d/t per Equation (B.2) at $w = 0.0096$ gives $\frac{N_r T d}{M_c} = 0.1500$, reported in Table B.1.

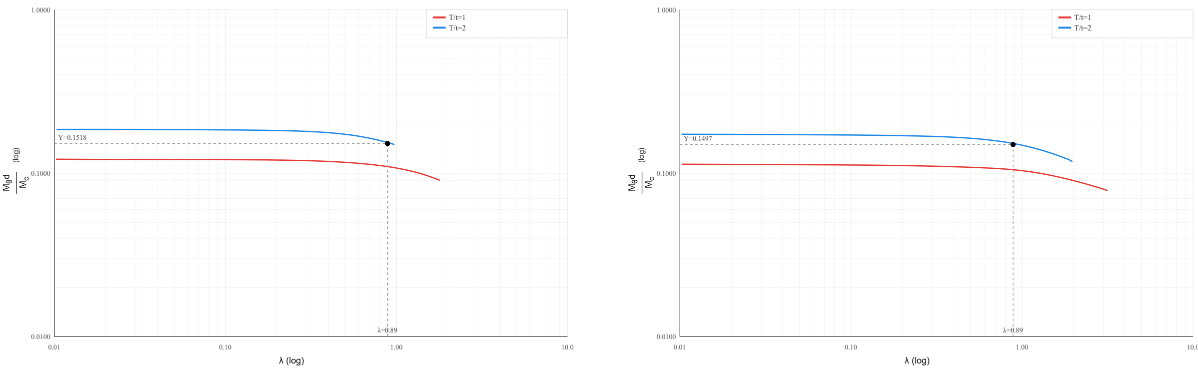

(a) (b)

Figure B.7 WRC 297 chart read for $\frac{M_\theta d}{M_c}$ (a) $d/t =$ 10.0000 (b) $d/t =$ 30.0000

At $T/t = 1.9500$, $d/t = 20.0960$ and $\lambda = 0.8870$, $\frac{M_\theta d}{M_c}$ is read on the two bracketing figures plotted above: Figure 32 at $d/t = 10.0000$ gives 0.1518 (Figure B.7(a)), and Figure 33 at $d/t = 30.0000$ gives 0.1497 (Figure B.7(b)), each after the T/t interpolation of Equation (B.1). Interpolating linearly across d/t per Equation (B.2) at $w = 0.5048$ gives $\frac{M_\theta d}{M_c} = 0.1508$, reported in Table B.1.

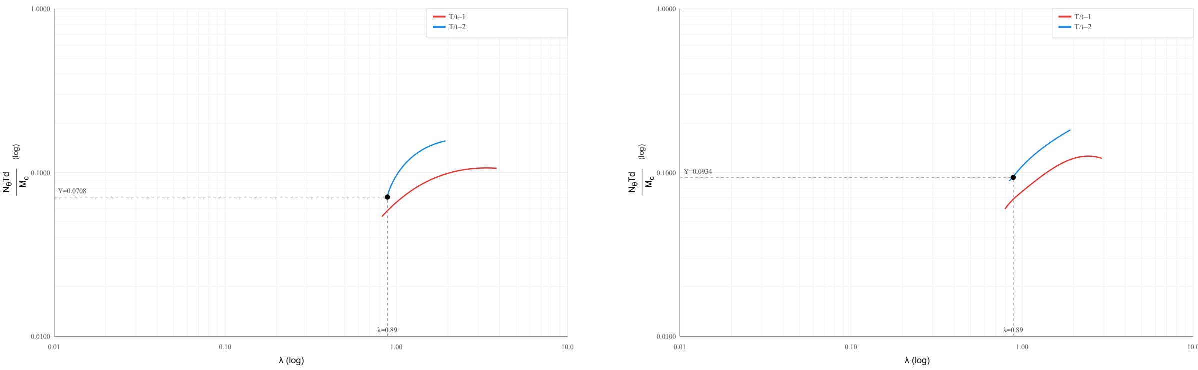

(a) (b)

Figure B.8 WRC 297 chart read for $\frac{N_\theta T d}{M_c}$ (a) $d/t =$ 20.0000 (b) $d/t =$ 30.0000

At $T/t = 1.9500$, $d/t = 20.0960$ and $\lambda = 0.8870$, $\frac{N_\theta T d}{M_c}$ is read on the two bracketing figures plotted above: Figure 37 at $d/t = 20.0000$ gives 0.0708 (Figure B.8(a)), and Figure 38 at $d/t = 30.0000$ gives 0.0934 (Figure B.8(b)), each after the T/t interpolation of Equation (B.1). Interpolating linearly across d/t per Equation (B.2) at $w = 0.0096$ gives $\frac{N_\theta T d}{M_c} = 0.0710$, reported in Table B.1.

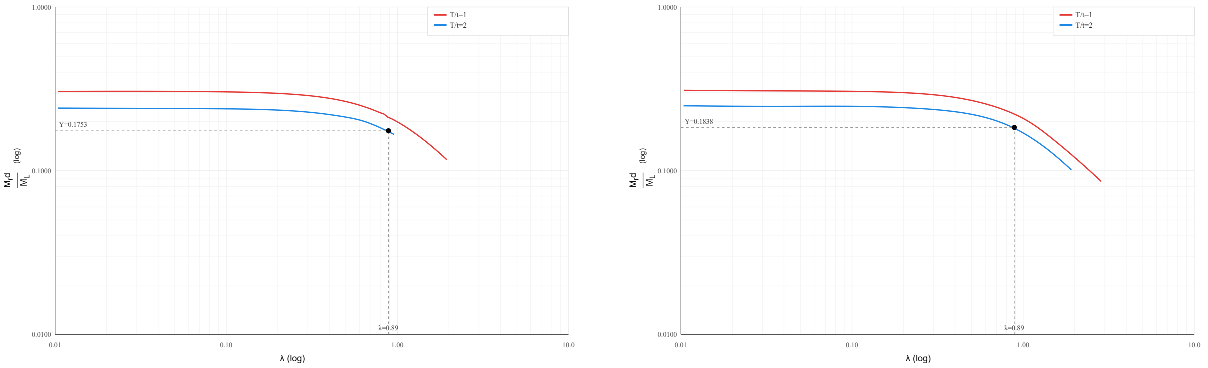

(a) **(b)**

Figure B.9 WRC 297 chart read for $\frac{M_r d}{M_L}$ (a) $d/t =$ 10.0000 (b) $d/t =$ 30.0000

At $T/t = 1.9500$, $d/t = 20.0960$ and $\lambda = 0.8870$, $\frac{M_r d}{M_L}$ is read on the two bracketing figures plotted above: Figure 41 at $d/t = 10.0000$ gives 0.1753 (Figure B.9(a)), and Figure 42 at $d/t = 30.0000$ gives 0.1838 (Figure B.9(b)), each after the T/t interpolation of Equation (B.1). Interpolating linearly across d/t per Equation (B.2) at $w = 0.5048$ gives $\frac{M_r d}{M_L} = 0.1796$, reported in Table B.1.

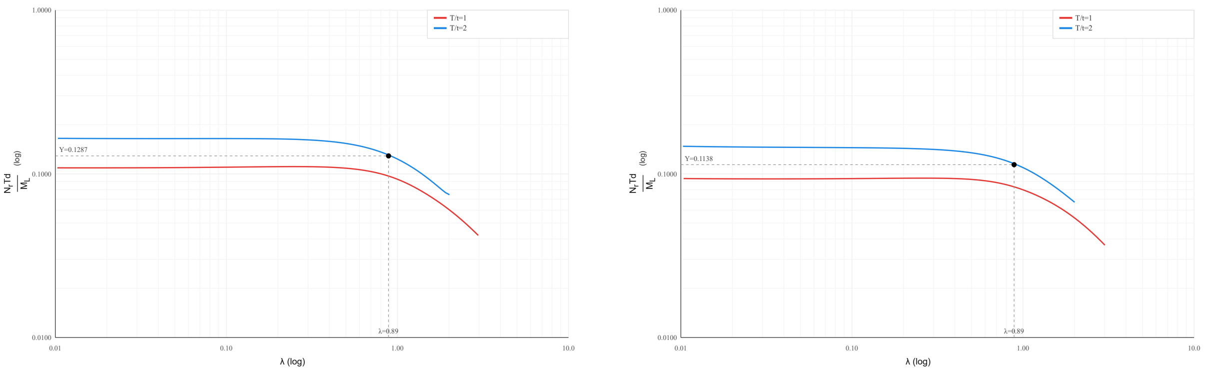

(a) **(b)**

Figure B.10 WRC 297 chart read for $\frac{N_r T d}{M_L}$ (a) $d/t =$ 20.0000 (b) $d/t =$ 30.0000

At $T/t = 1.9500$, $d/t = 20.0960$ and $\lambda = 0.8870$, $\frac{N_r T d}{M_L}$ is read on the two bracketing figures plotted above: Figure 46 at $d/t = 20.0000$ gives 0.1287 (Figure B.10(a)), and Figure 47 at $d/t = 30.0000$ gives 0.1138 (Figure B.10(b)), each after the T/t interpolation of Equation (B.1). Interpolating linearly across d/t per Equation (B.2) at $w = 0.0096$ gives $\frac{N_r T d}{M_L} = 0.1286$, reported in Table B.1.

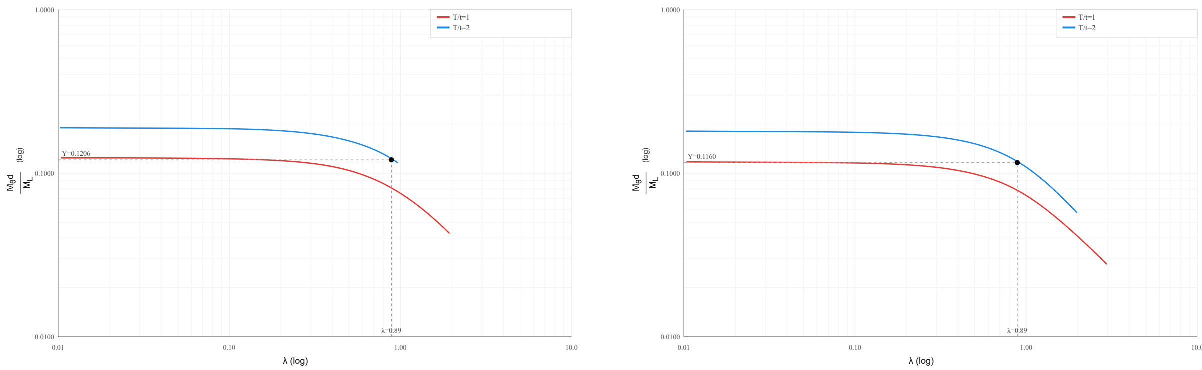

(a) **(b)**

Figure B.11 WRC 297 chart read for $\frac{M_\theta d}{M_L}$ (a) $d/t =$ 10.0000 (b) $d/t =$ 30.0000

At $T/t = 1.9500$, $d/t = 20.0960$ and $\lambda = 0.8870$, $\frac{M_\theta d}{M_L}$ is read on the two bracketing figures plotted above: Figure 50 at $d/t = 10.0000$ gives 0.1206 (Figure B.11(a)), and Figure 51 at $d/t = 30.0000$ gives 0.1160 (Figure B.11(b)), each after the T/t interpolation of Equation (B.1). Interpolating linearly across d/t per Equation (B.2) at $w = 0.5048$ gives $\frac{M_\theta d}{M_L} = 0.1183$, reported in Table B.1.

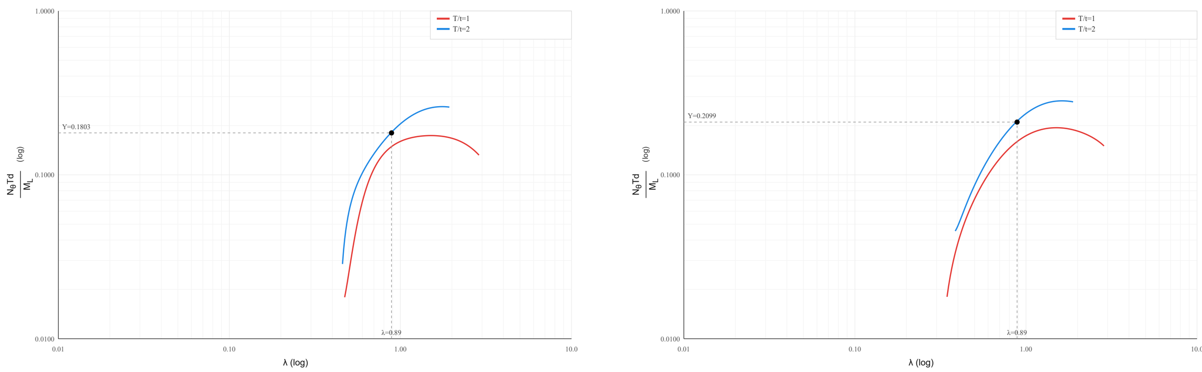

(a) **(b)**

Figure B.12 WRC 297 chart read for $\frac{N_\theta T d}{M_L}$ (a) $d/t =$ 20.0000 (b) $d/t =$ 30.0000

At $T/t = 1.9500$, $d/t = 20.0960$ and $\lambda = 0.8870$, $\frac{N_\theta T d}{M_L}$ is read on the two bracketing figures plotted above: Figure 55 at $d/t = 20.0000$ gives 0.1803 (Figure B.12(a)), and Figure 56 at $d/t = 30.0000$ gives 0.2099 (Figure B.12(b)), each after the T/t interpolation of Equation (B.1). Interpolating linearly across d/t per Equation (B.2) at $w = 0.0096$ gives $\frac{N_\theta T d}{M_L} = 0.1805$, reported in Table B.1.

B.1.3 Stress Summary

Table B.1 WRC 297 stress summary at T/t=1.9500, d/t=20.0960

Name	Value
$\frac{M_r}{F}$	0.1448
$\frac{N_r T}{F}$	0.1111
$\frac{M_\theta}{F}$	0.0866
$\frac{N_\theta T}{F}$	0.1758
$\frac{M_r d}{M_c}$	0.2242
$\frac{N_r T d}{M_c}$	0.1500
$\frac{M_\theta d}{M_c}$	0.1508
$\frac{N_\theta T d}{M_c}$	0.0710
$\frac{M_r d}{M_L}$	0.1796
$\frac{N_r T d}{M_L}$	0.1286
$\frac{M_\theta d}{M_L}$	0.1183
$\frac{N_\theta T d}{M_L}$	0.1805

B.2 Coefficient Extraction from WRC 537 Charts

B.2.1 Interpolation Rules

The WRC 537 influence coefficient charts are evaluated using the following rule:

1. **Within a figure (varying γ):** use logarithmic interpolation in γ; fall back to linear if any of γ, γ_1, γ_2 are non-positive (≤ 0). With γ,

$$Y(\gamma, d) = y_1 + (y_2 - y_1)\,\frac{\ln\gamma - \ln\gamma_1}{\ln\gamma_2 - \ln\gamma_1} \tag{B.3}$$

   Fallback (linear): $Y(\gamma, d) = y_1 + (y_2 - y_1)\,\frac{\gamma-\gamma_1}{\gamma_2-\gamma_1}$.
   If $\gamma = \gamma_1 = \gamma_2$, use the exact value $Y(\gamma, d) = \gamma$.

Extrapolation Extrapolation outside the line ranges is strictly not permitted per WRC 297 and WRC 537.

B.2.2 Worked Chart Read

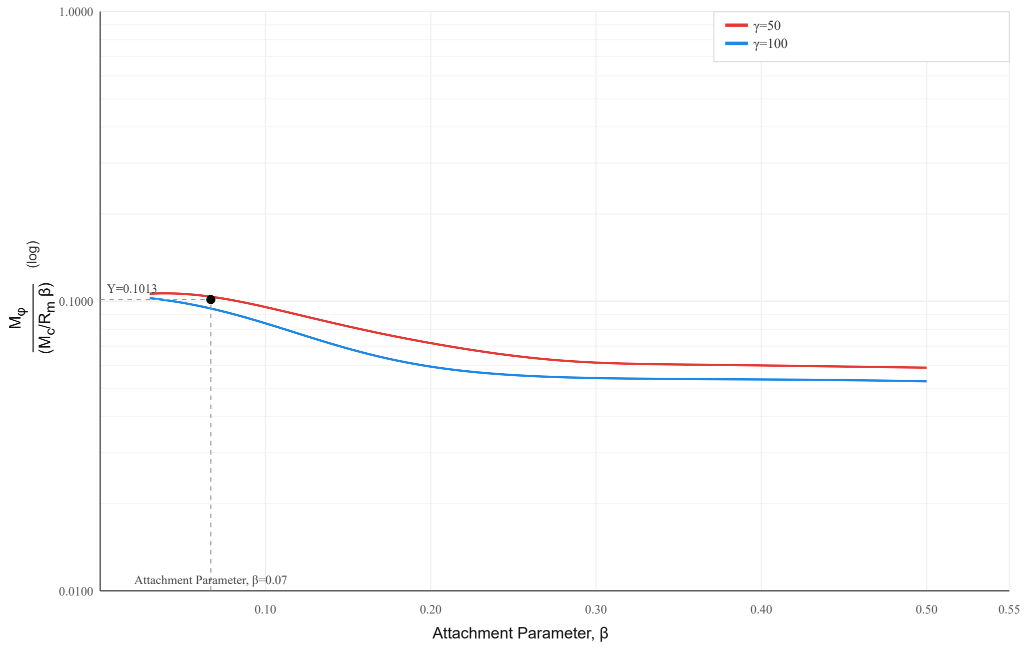

Figure B.13 WRC 537 Figure 1A at β=0.0669, γ=60

As shown in Figure B.13, $\frac{M_\phi}{M_c/(R_m\beta)} = 0.1013$ at $\beta = 0.0669$, per Equation (B.3); see Table B.2 for the full results summary.

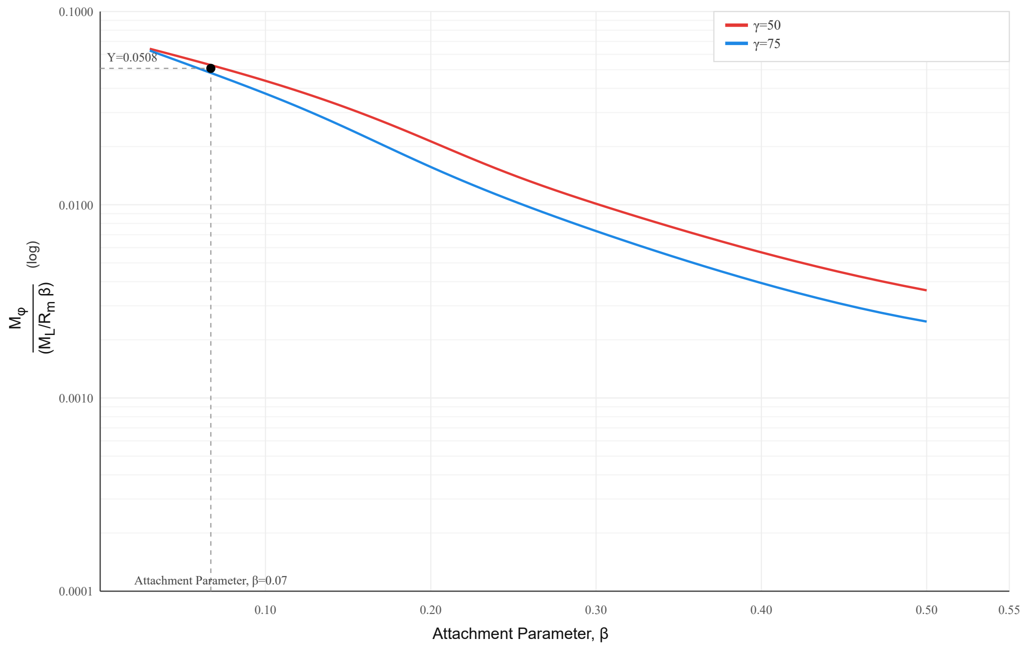

Figure B.14 WRC 537 Figure 1B at β=0.0669, γ=60

As shown in Figure B.14, $\frac{M_\phi}{M_L/(R_m\beta)} = 0.0508$ at $\beta = 0.0669$, per Equation (B.3); see Table B.2

for the full results summary.

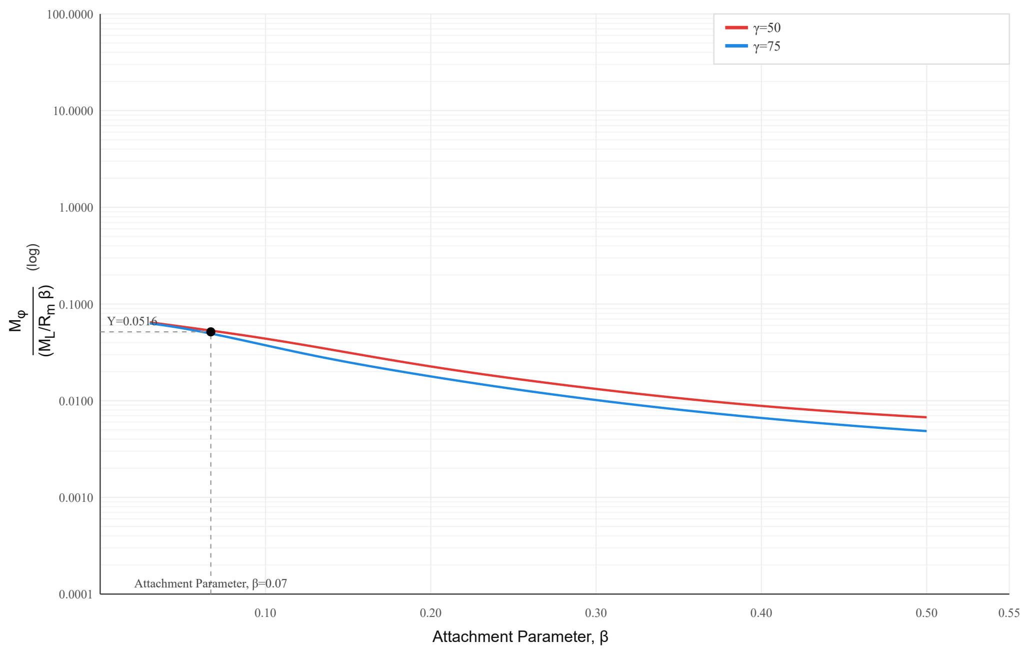

Figure B.15 WRC 537 Figure 1B-1 at β=0.0669, γ=60

As shown in Figure B.15, $\frac{M_\phi}{M_L/(R_m\beta)} = 0.0516$ at $\beta = 0.0669$, per Equation (B.3); see Table B.2 for the full results summary.

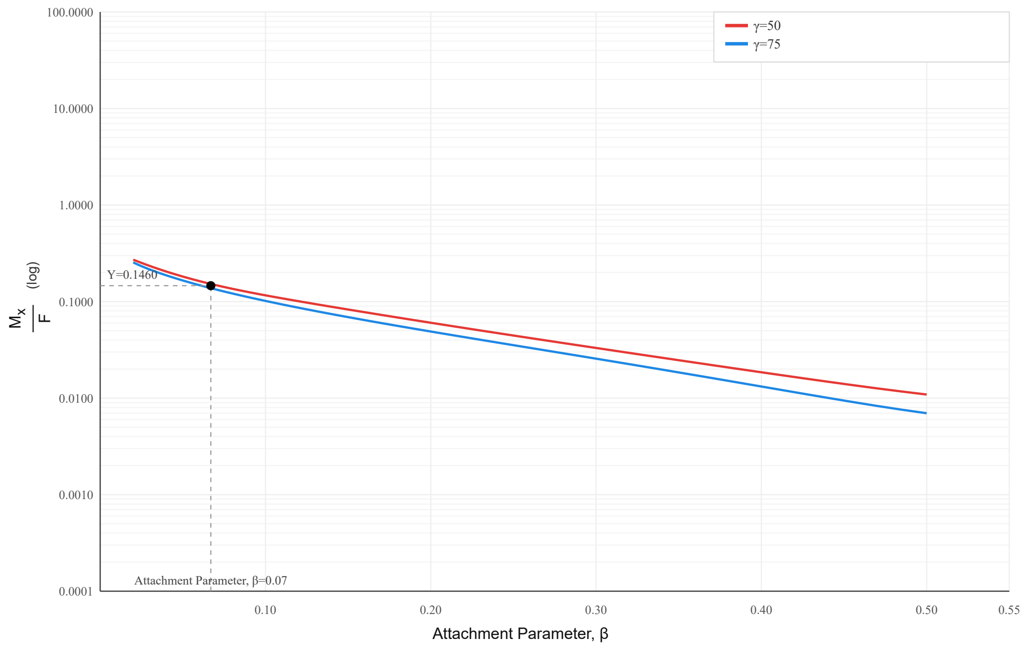

Figure B.16 WRC 537 Figure 1C-1 at β=0.0669, γ=60

As shown in Figure B.16, $\frac{M_x}{F} = 0.1460$ at $\beta = 0.0669$, per Equation (B.3); see Table B.2 for the full results summary.

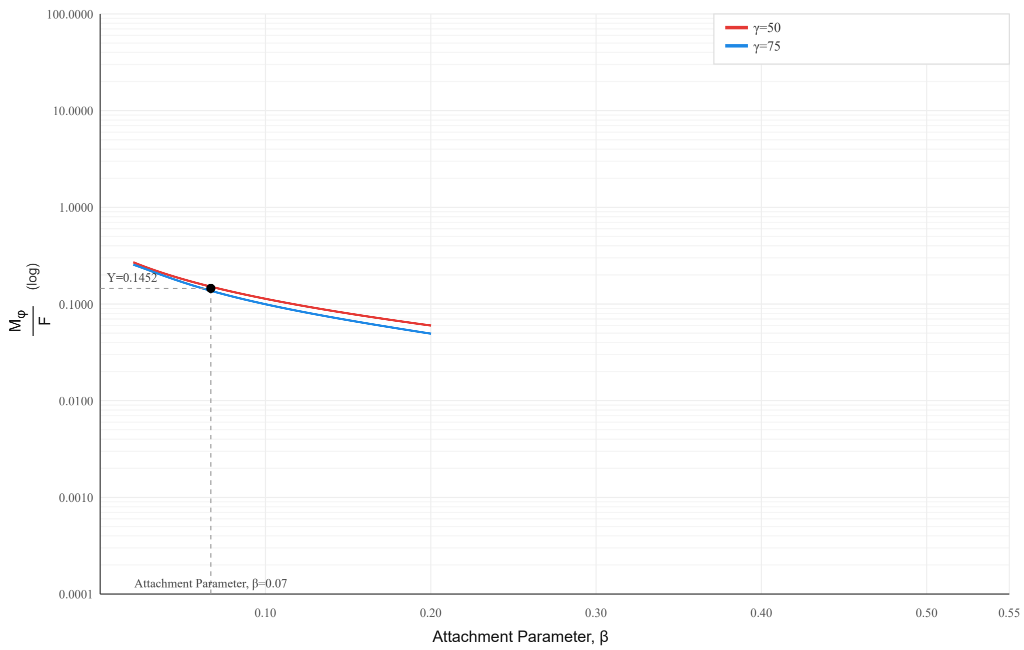

Figure B.17 WRC 537 Figure 1C (points C, D) at β=0.0669, γ=60

As shown in Figure B.17, $\frac{M_\phi}{F}$ = 0.1452 at β = 0.0669, per Equation (B.3); see Table B.2 for the full results summary.

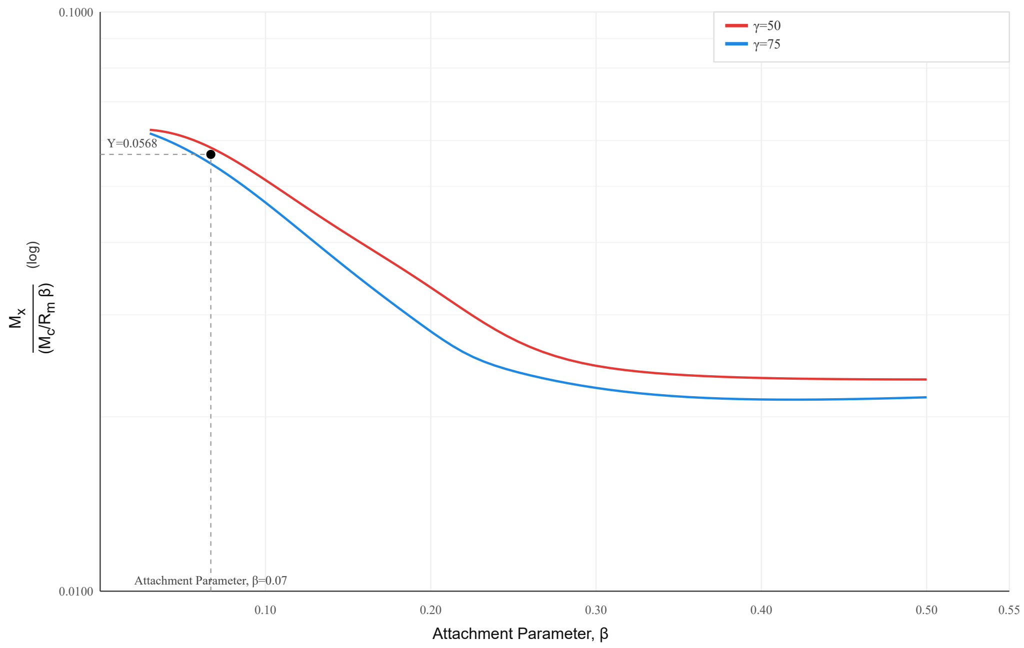

Figure B.18 WRC 537 Figure 2A at β=0.0669, γ=60

As shown in Figure B.18, $\frac{M_x}{M_c/(R_m\beta)}$ = 0.0568 at β = 0.0669, per Equation (B.3); see Table B.2

for the full results summary.

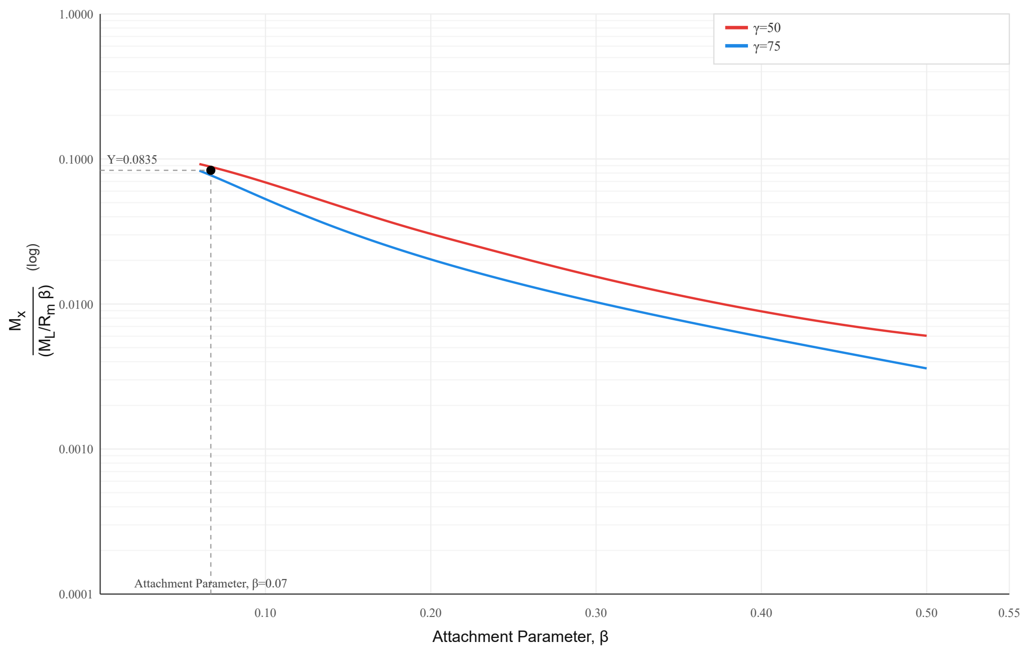

Figure B.19 WRC 537 Figure 2B at β=0.0669, γ=60

As shown in Figure B.19, $\frac{M_x}{M_L/(R_m\beta)} = 0.0835$ at $\beta = 0.0669$, per Equation (B.3); see Table B.2 for the full results summary.

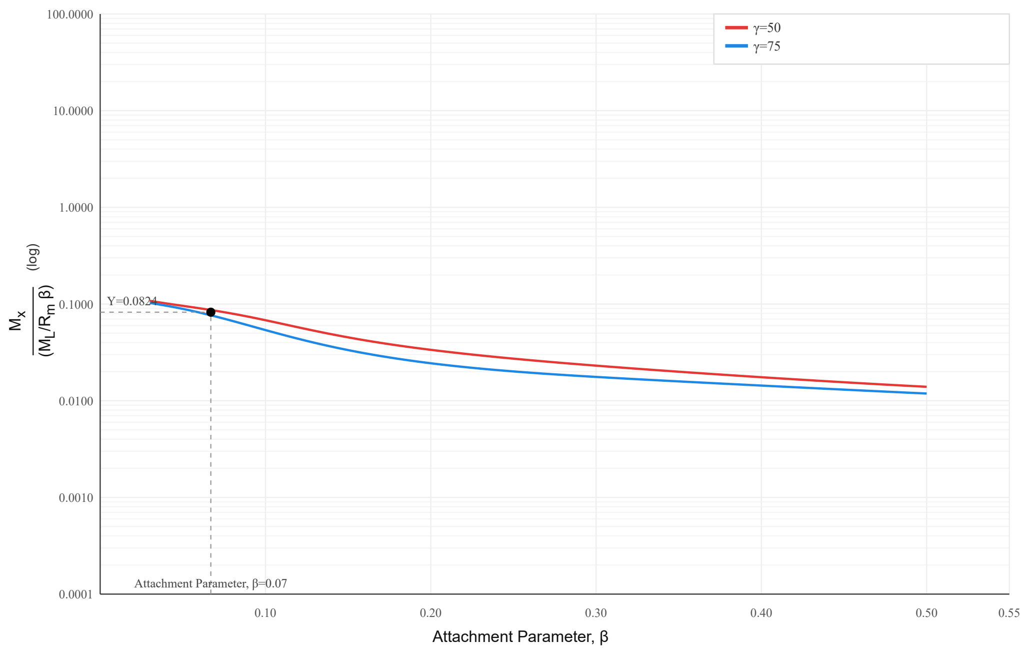

Figure B.20 WRC 537 Figure 2B-1 at β=0.0669, γ=60

As shown in Figure B.20, $\frac{M_x}{M_L/(R_m\beta)} = 0.0824$ at $\beta = 0.0669$, per Equation (B.3); see Table B.2

for the full results summary.

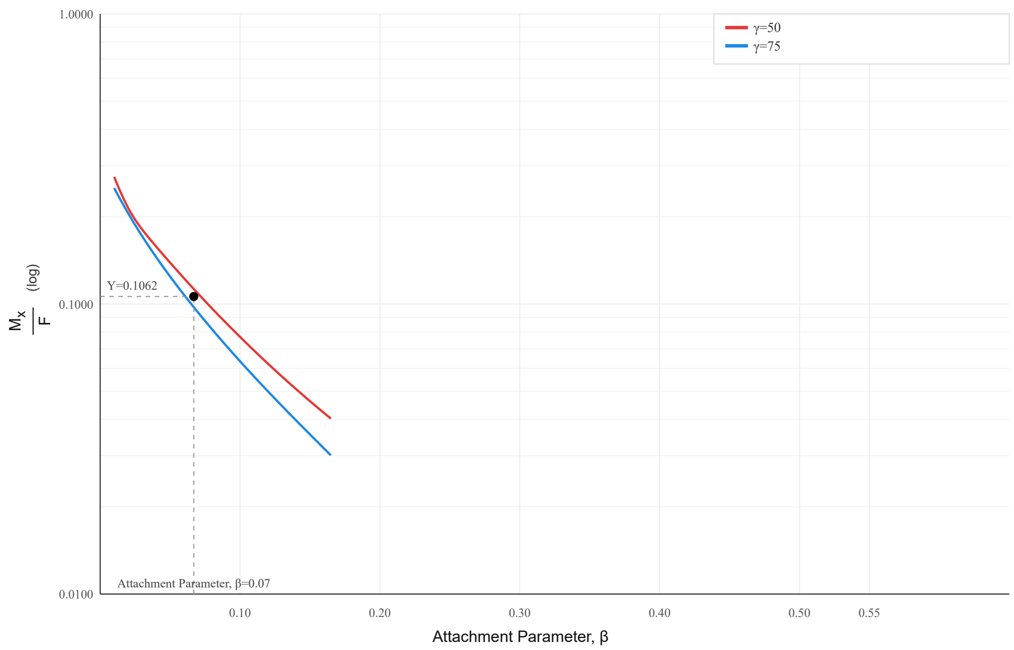

Figure B.21 WRC 537 Figure 2C at β=0.0669, γ=60

As shown in Figure B.21, $\frac{M_x}{F}$ = 0.1062 at β = 0.0669, per Equation (B.3); see Table B.2 for the full results summary.

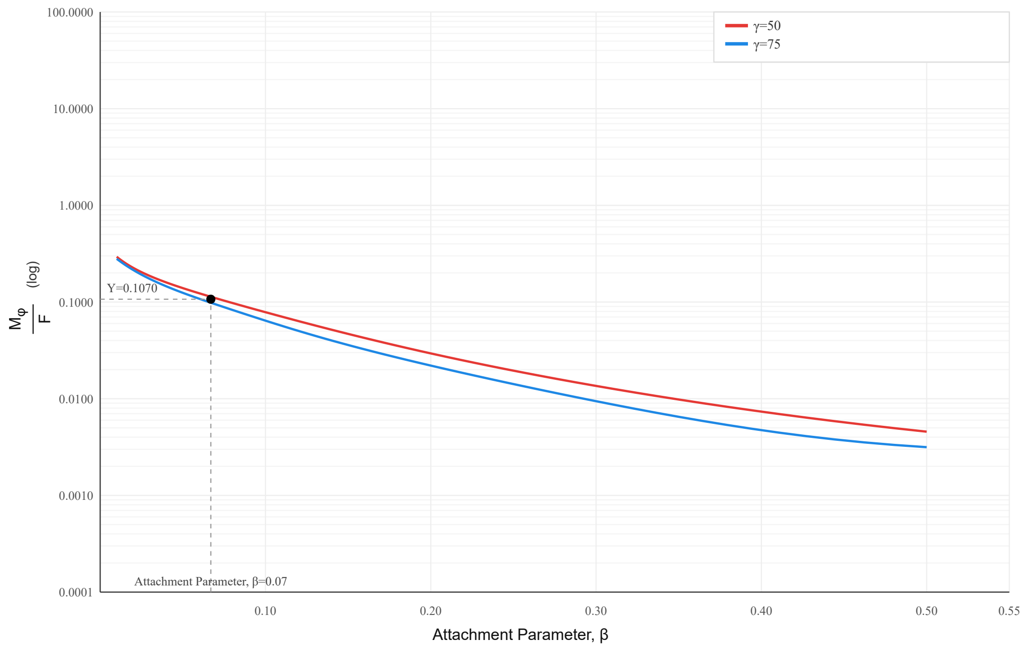

Figure B.22 WRC 537 Figure 2C-1 (points A, B) at β=0.0669, γ=60

As shown in Figure B.22, $\frac{M_\phi}{F}$ = 0.1070 at β = 0.0669, per Equation (B.3); see Table B.2 for the full results summary.

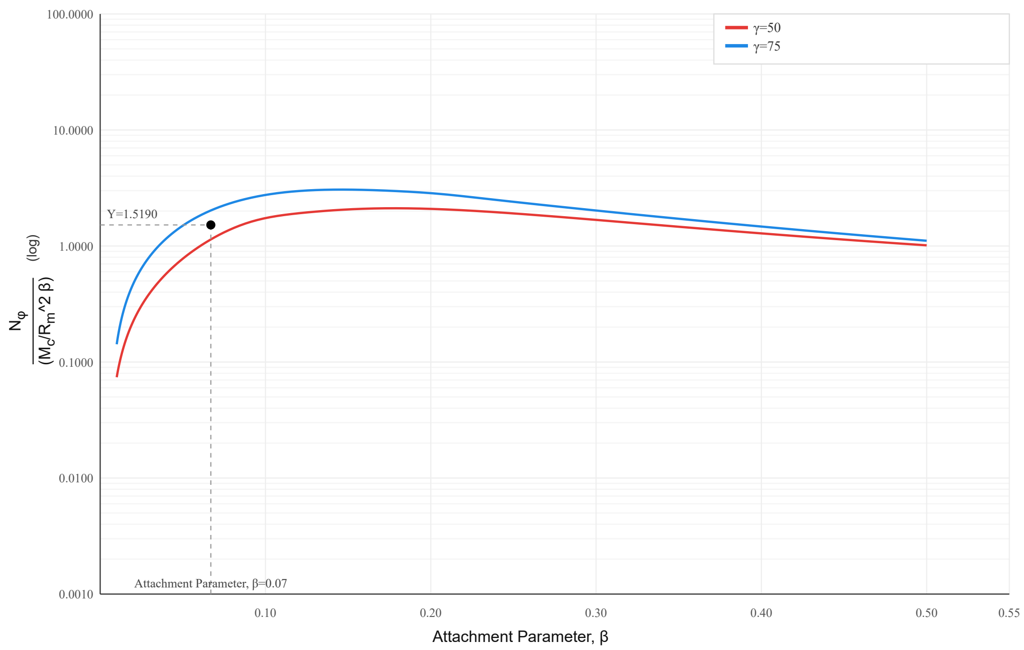

Figure B.23 WRC 537 Figure 3A at β=0.0669, γ=60

As shown in Figure B.23, $\frac{N_\phi}{M_c/(R_m^2\beta)} = 1.5190$ at $\beta = 0.0669$, per Equation (B.3); see Table B.2 for the full results summary.

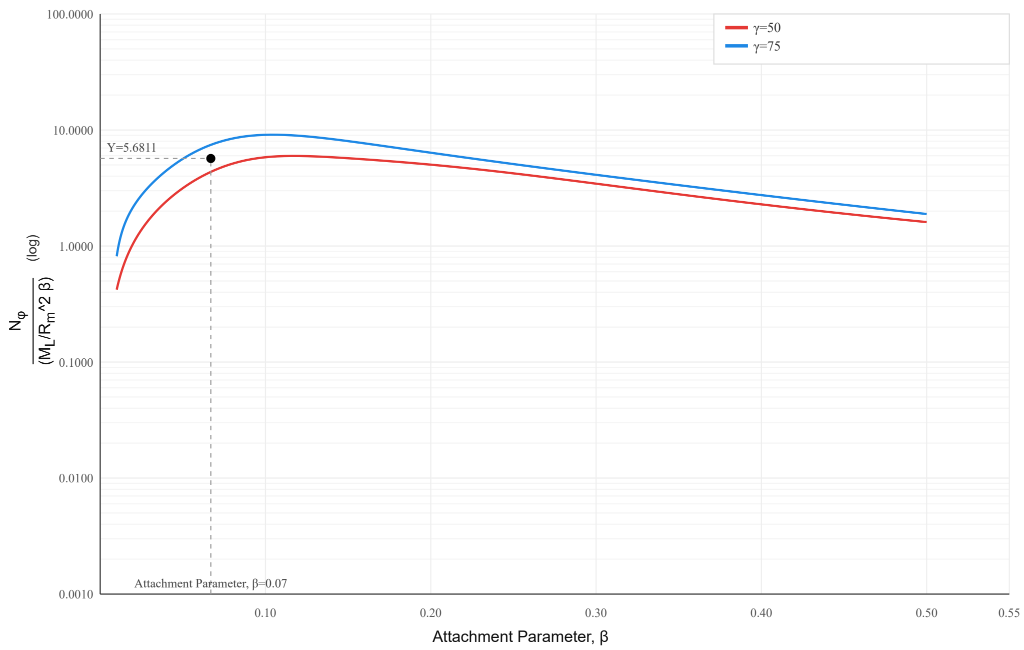

Figure B.24 WRC 537 Figure 3B at β=0.0669, γ=60

As shown in Figure B.24, $\frac{N_\phi}{M_L/(R_m^2\beta)} = 5.6811$ at $\beta = 0.0669$, per Equation (B.3); see Table B.2

for the full results summary.

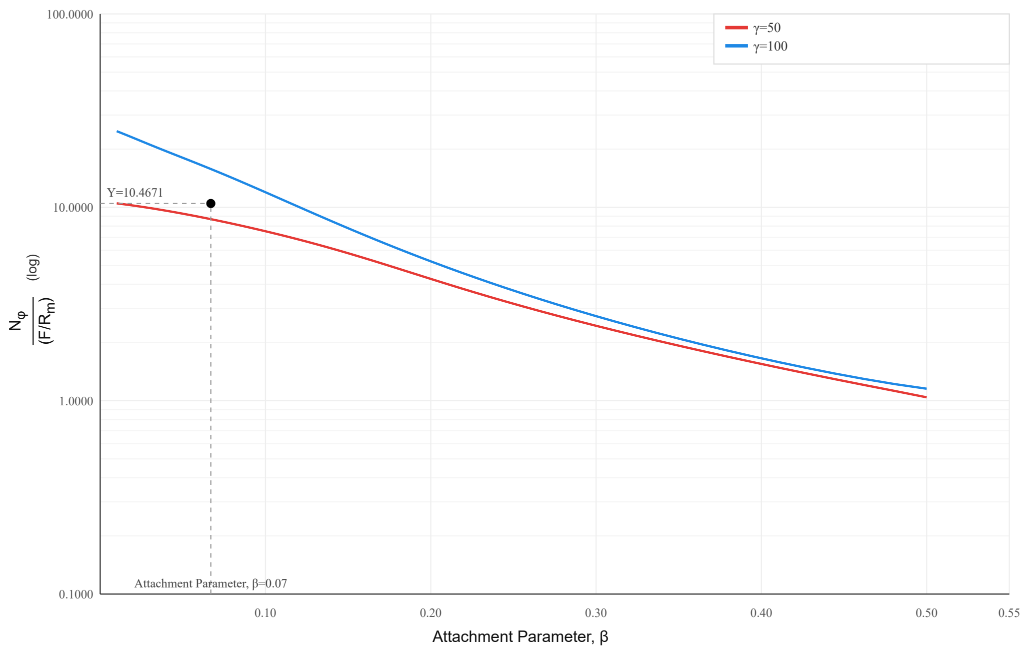

Figure B.25 WRC 537 Figure 3C at β=0.0669, γ=60

As shown in Figure B.25, $\frac{N_\phi}{F/R_m} = 10.4671$ at $\beta = 0.0669$, per Equation (B.3); see Table B.2 for the full results summary.

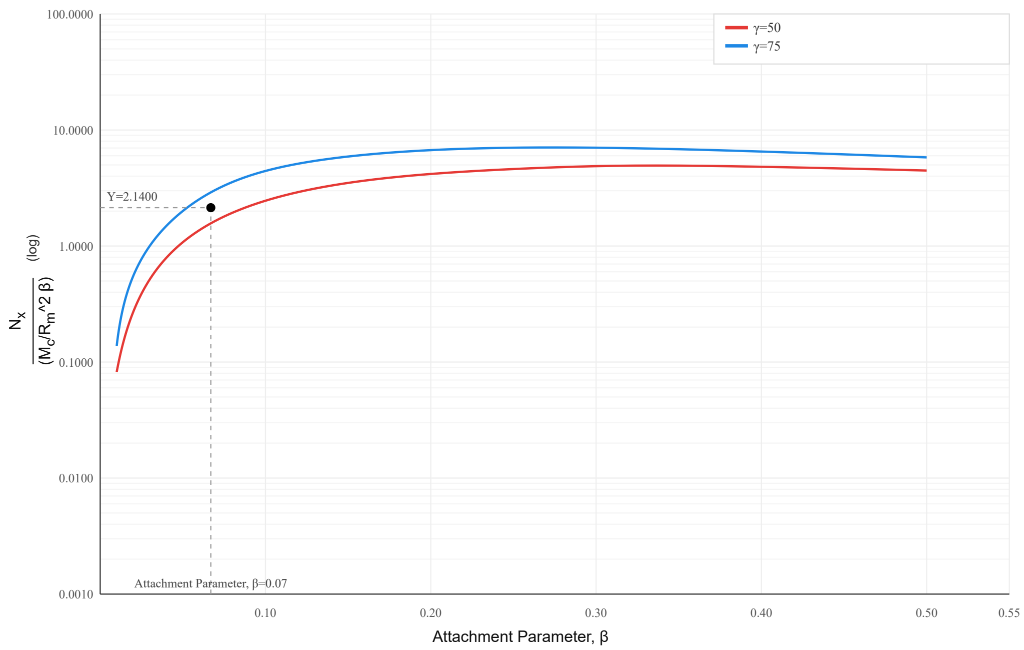

Figure B.26 WRC 537 Figure 4A at β=0.0669, γ=60

As shown in Figure B.26, $\frac{N_x}{M_c/(R_m^2\beta)} = 2.1400$ at $\beta = 0.0669$, per Equation (B.3); see Table B.2

for the full results summary.

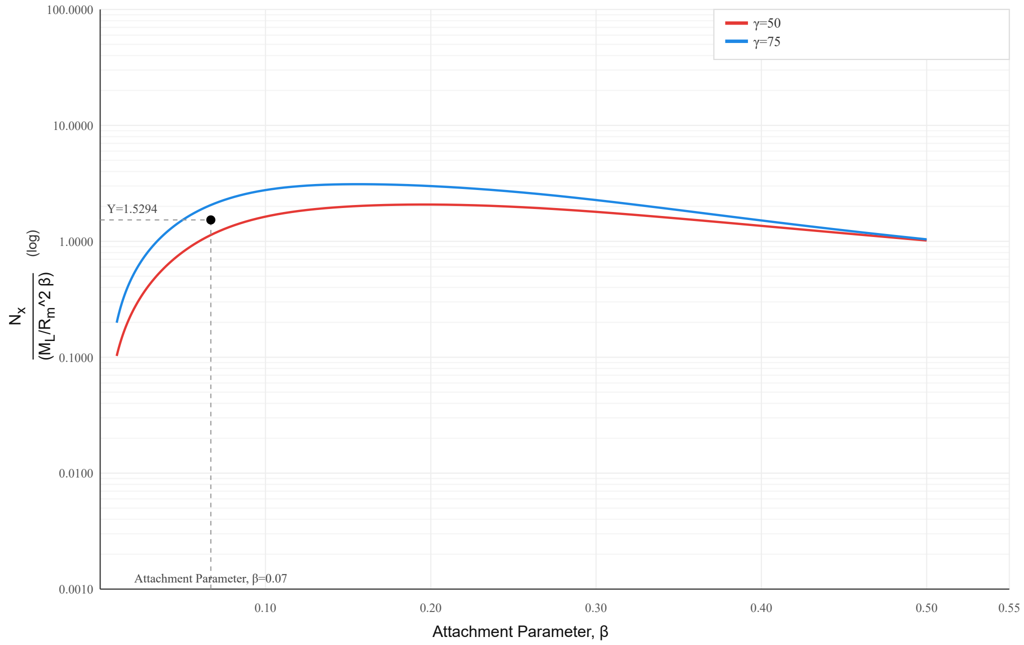

Figure B.27 WRC 537 Figure 4B at β=0.0669, γ=60

As shown in Figure B.27, $\frac{N_x}{M_L/(R_m^2\beta)} = 1.5294$ at $\beta = 0.0669$, per Equation (B.3); see Table B.2 for the full results summary.

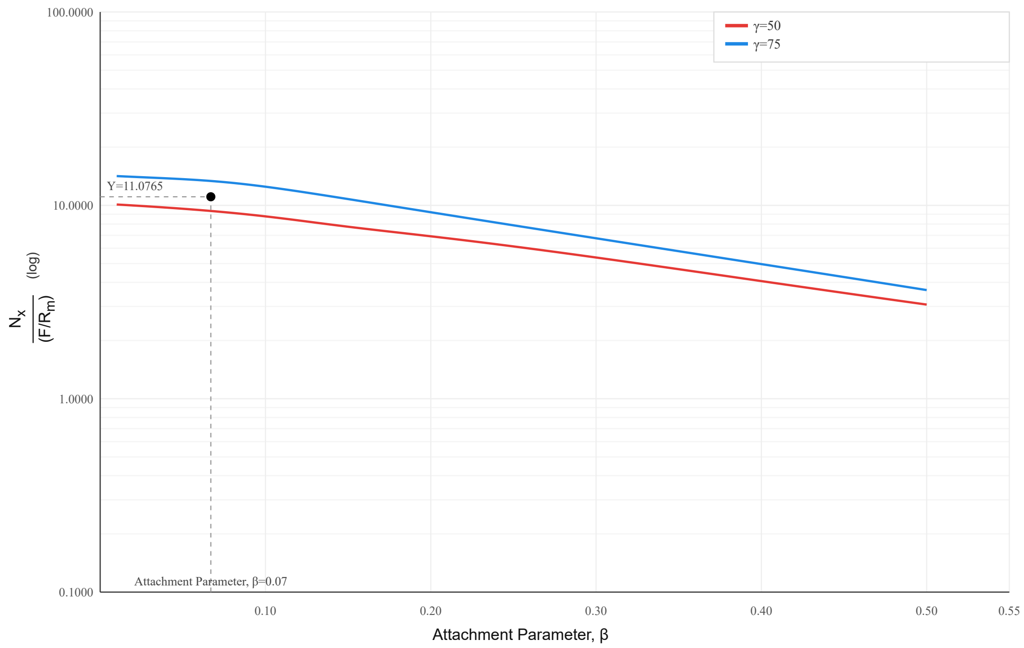

Figure B.28 WRC 537 Figure 4C at β=0.0669, γ=60

As shown in Figure B.28, $\frac{N_x}{F/R_m} = 11.0765$ at $\beta = 0.0669$, per Equation (B.3); see Table B.2

for the full results summary.

B.2.3 Stress Summary

Table B.2 WRC 537 stress summary

Name	Value
Figure 1A: $\frac{M_\phi}{M_c/(R_m\beta)}$	0.1013
Figure 1B: $\frac{M_\phi}{M_L/(R_m\beta)}$	0.0508
Figure 1B-1: $\frac{M_\phi}{M_L/(R_m\beta)}$	0.0516
Figure 1C-1: $\frac{M_x}{F}$	0.1460
Figure 1C (points C, D): $\frac{M_\phi}{F}$	0.1452
Figure 2A: $\frac{M_x}{M_c/(R_m\beta)}$	0.0568
Figure 2B: $\frac{M_x}{M_L/(R_m\beta)}$	0.0835
Figure 2B-1: $\frac{M_x}{M_L/(R_m\beta)}$	0.0824
Figure 2C: $\frac{M_x}{F}$	0.1062
Figure 2C-1 (points A, B): $\frac{M_\phi}{F}$	0.1070
Figure 3A: $\frac{N_\phi}{M_c/(R_m^2\beta)}$	1.5190
Figure 3B: $\frac{N_\phi}{M_L/(R_m^2\beta)}$	5.6811
Figure 3C: $\frac{N_\phi}{F/R_m}$	10.4671
Figure 4A: $\frac{N_x}{M_c/(R_m^2\beta)}$	2.1400
Figure 4B: $\frac{N_x}{M_L/(R_m^2\beta)}$	1.5294
Figure 4C: $\frac{N_x}{F/R_m}$	11.0765

C. Example Calculation

C.1 Pressure coefficient calculations as per PVP vol. 399

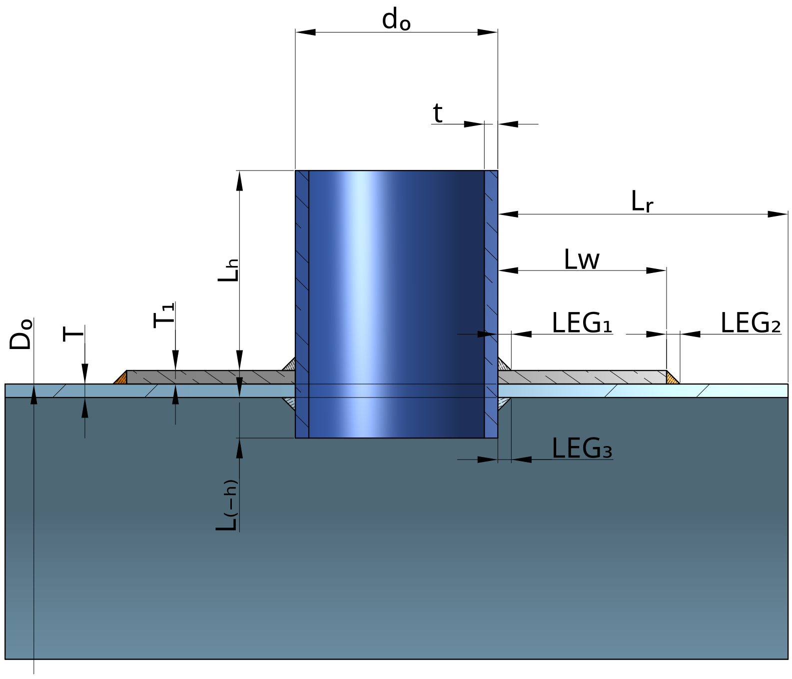

Figure C.1 Nozzle geometry for internal-pressure coefficient calculations

Overview of Intensification Factor Model:

The factors below are the Bildy pressure-area balance (PVP vol. 399, Eqs. (1)–(19)). Lengths that carry load are corroded: $T_{eff} = T - c_{shell}$ is the shell wall and $t_{eff} = t - c_{nozzle}$ the nozzle wall, while D_i, d_i and t are the nominal dimensions and $D_i + 2c_{shell}$, $d_i + 2c_{nozzle}$ the corroded bores the pressure acts on. T_1 is the pad thickness, l_2 the pad radial width, l_3 and s_3 the inside-projection length and wall thickness, and Δ, Δ_1, Δ_2 the base, nozzle and pad weld legs. Terms belonging to a detail the junction does not have are zero.

Equivalent Shell Length Definition:

$$L_{eq} = \min\left\{8\,T_{eff},\ 2\sqrt{0.5\,D_i\,T_{eff}}\right\} \tag{C.1}$$

Equivalent Nozzle Extrusion Length:

$$L_{h,eq} = \min\left\{8\,T_{eff},\ T_{eff} + T_1 + 0.55\sqrt{d_i\,t_{eff}} + 0.5\,\Delta\right\} \tag{C.2}$$

Equivalent Cover Plate Length:

$$L_{w,eq} = \min\{\,l_2,\ L_{h,eq}\,\} \tag{C.3}$$

Equivalent Nozzle Inner Extrusion Length:

$$L_{(-h),eq} = \min\left\{l_3,\ 8\,(T_{eff} + T_1),\ 0.55\,\sqrt{d_i\,(s_3 - 2\,c_{nozzle})} + 0.5\,\Delta_2\right\} \tag{C.4}$$

Total reinforcing area A_T (Bildy Eq. (18); the weld throats are $0.5\,\mathrm{Leg}^2$, the 45° fillet triangle, per Bildy Eqs. (9)–(11)):

$$A_T = L_{eq}\,T_{eff} + L_{h,eq}\,t_{eff} + L_{w,eq}\,T_1 + L_{(-h),eq}\,(s_3 - 2\,c_{nozzle}) + 0.5\left(\Delta^2 + \Delta_1^2 + \Delta_2^2\right) \tag{C.5}$$

Circumferential (longitudinal-section) Stress Intensification Factor for Internal Pressure:

$$I_{\theta,p} = \frac{2\left(T_{eff} + T_1\right)\left[(d_i + 2c_{nozzle})\left(L_{h,eq} - c_{nozzle}\right) + (D_i + 2c_{shell})\left(L_{eq} + t + 0.5\,d_i\right)\right]}{\left[D_i + \left(T_{eff} + T_1\right)\right]\,A_T} - 1 \tag{C.6}$$

Radial (cross-section) Stress Intensification Factor for Internal Pressure — the same balance, with the nozzle pressure-area term counted twice:

$$I_{r,p} = \frac{2\left(T_{eff} + T_1\right)\left[2\,(d_i + 2c_{nozzle})\left(L_{h,eq} - c_{nozzle}\right) + (D_i + 2c_{shell})\left(L_{eq} + t + 0.5\,d_i\right)\right]}{\left[D_i + \left(T_{eff} + T_1\right)\right]\,A_T} - 1 \tag{C.7}$$

d_i is clamped so that the nozzle slenderness d_o/t_{eff} stays inside the WRC 297 §3.2 published band $10 \le d_o/t_{eff} \le 100$; for in-band geometries the clamp is inert. Both factors are rounded to three decimal places before use.

Pressure Coefficient Formulations:

$$k_{\theta,p} = \begin{cases} 0.5 + 0.5\,I_{\theta,p}, & I_{\theta,p} < 1 \\ I_{\theta,p}, & I_{\theta,p} \ge 1 \end{cases} \tag{C.8}$$

$$k_{r,p} = \begin{cases} 0.5 + 0.5\,I_{r,p}, & I_{r,p} < 1 \\ I_{r,p}, & I_{r,p} \ge 1 \end{cases} \tag{C.9}$$

C.2 Nozzle Pressure and Example Calculation

The following sub-sections set out the WRC 297 nozzle-stress equations used in this report and identify the chart each coefficient is read from. The final sub-section works the equations through with this design's own numbers at the governing point.

In the load-stress equations below the shell wall T, the nozzle wall t and the shell mean radius R_m are the *corroded* values $T - c_{shell}$, $t - c_{nozzle}$ and $R_m + c_{shell}/2$ — the condition the chart reads and the resulting stresses are evaluated in (ASME BPVC.VIII.2 §4.1.4.1: dimensional symbols in design equations represent the corroded condition). The internal-pressure terms carry their own bases, stated with each equation.

C.2.1 Circumferential stresses, σ_θ

Circumferential membrane stresses (points A_u to D_L) of external force F:

$$\sigma_{\theta,m}(F) = \left(\frac{N_\theta\, T}{F}\right)\frac{F}{T^2} \tag{C.10}$$

Coefficient from Figure B.4. The chart value $N_\theta T/F$ is dimensionless, so the load group is F/T^2 — the membrane force per unit length N_θ divided once more by T to give a stress. This is the same form as the M_C and M_L equations below.

Circumferential membrane stresses (points C_u to D_L) from M_C moment:

$$\sigma_{\theta,m}(M_C) = \left(\frac{N_\theta T\, d}{M_C}\right)\frac{M_C}{T^2\, d_o} \tag{C.11}$$

Coefficient from Figure B.8.
Note: WRC 297 gives the nozzle no circumferential *bending* term. §3.1 states that "nozzle circumferential bending stresses are assumed to be negligible compared with the membrane stresses" and then gives Eqs. (7) and (8), which carry n_θ alone; the $\pm 6\, m_\theta$ form belongs to Eqs. (2) and (4), which apply to the vessel shell. Table 2 repeats the exclusion. The nozzle's total circumferential stress is therefore its membrane stress (see Equations (C.18) and (C.19)).

Circumferential membrane stresses (points A_u to B_L) from M_L moment:

$$\sigma_{\theta,m}(M_L) = \left(\frac{N_\theta T\, d}{M_L}\right)\frac{M_L}{T^2\, d_o} \tag{C.12}$$

Coefficient from Figure B.12.

Circumferential stress (points A_u to B_L) due to internal pressure:

$$\sigma_{\theta,p} = k_{\theta,p}\,\frac{p\, D_m}{2\, T} \tag{C.13}$$

Where $k_{\theta p}$ is the pressure coefficient defined in the internal pressure section above (see Eq. (C.8)).

Circumferential stress (points C_u to D_L) due to internal pressure:

$$\sigma_{\theta p} = \frac{p\, D_m}{2\, T} \tag{C.14}$$

General membrane circumferential stresses (points A_u to D_L) due to pressure:

$$P_{\theta,m} = \frac{p\, D_m}{2\, T} \tag{C.15}$$

Total membrane circumferential stresses (points A_u to B_L):

$$\sigma_{\theta,m} = \sigma_{\theta,m}(F) + \sigma_{\theta,m}(M_L) + \sigma_{\theta p} \tag{C.16}$$

Total membrane circumferential stresses (points C_u to D_L):

$$\sigma_{\theta,m} = \sigma_{\theta,m}(F) + \sigma_{\theta,m}(M_C) + \sigma_{\theta p} \tag{C.17}$$

Total circumferential stresses (points A_u to B_L). With no nozzle bending term, the total equals the membrane total above:

$$\sigma_\theta = \sigma_{\theta,m}(F) + \sigma_{\theta,m}(M_L) + \sigma_{\theta p} \tag{C.18}$$

Total circumferential stresses (points C_u to D_L):

$$\sigma_\theta = \sigma_{\theta,m}(F) + \sigma_{\theta,m}(M_C) + \sigma_{\theta p} \tag{C.19}$$

C.2.2 Longitudinal stresses, σ_r

Longitudinal membrane stresses (points A_u to D_L) from external force F:

$$\sigma_{r,m}(F) = \frac{F}{A} \tag{C.20}$$

where

$$A = \frac{\pi}{4}\left(d_o^2 - d_i^2\right) \tag{C.21}$$

is the design cross-sectional area of the nozzle.

Longitudinal bending stresses (points A_u to D_L) from external force F:

$$\sigma_{r,b}(F) = \left(6\left(\frac{M_r}{F}\right) - 3\left(\frac{N_r T}{F}\right)\right)\frac{F}{t^2} \tag{C.22}$$

Coefficients from Figures B.1 and B.2.

Longitudinal membrane stresses (points C_u to D_L) from M_C moment:

$$\sigma_{r,m}(M_C) = \frac{M_C}{S}, \tag{C.23}$$

where

$$S = \frac{\pi\left(d_o^4 - d_i^4\right)}{32\, d_o} \tag{C.24}$$

is the design section modulus of the nozzle.

Longitudinal bending stresses (points C_u to D_L) from M_C moment:

$$\sigma_{r,b}(M_C) = \left(6\left(\frac{M_r\, d}{M_c}\right) - 3\left(\frac{N_r T\, d}{M_c}\right)\right)\frac{M_C}{t^2\, d_o} \tag{C.25}$$

Coefficients from Figures B.5 and B.6.

Longitudinal membrane stresses (points A_u to B_L) from M_L moment:

$$\sigma_{r,m}(M_L) = \frac{M_L}{S}, \tag{C.26}$$

where

$$S = \frac{\pi\left(d_o^4 - d_i^4\right)}{32\, d_o} \tag{C.27}$$

is the design section modulus of the nozzle.

Longitudinal bending stresses (points A_u to B_L) from M_L moment:

$$\sigma_{r,b}(M_L) = \left(6\left(\frac{M_r\,d}{M_L}\right) - 3\left(\frac{N_r T\,d}{M_L}\right)\right)\frac{M_L}{t^2\,d_o} \tag{C.28}$$

Coefficients from Figures B.9 and B.10.

Longitudinal stress (points A_u to D_L) due to internal pressure. This is a *nozzle-wall* axial membrane stress, so it is the end load $p\,\pi d_i^2/4$ carried by the nozzle metal area $\pi(d_o^2 - d_i^2)/4$ — not a shell D_m/T term — and no pressure intensification factor is applied to it:

$$\sigma_{r,p} = \frac{p\,d_i^2}{d_o^2 - d_i^2} \tag{C.29}$$

WRC 297 §3.1: after giving the approximate πdt area of Eq. (5), the Bulletin states that "for nozzles with smaller d/t ratios, the following exact expressions should be used" and gives $A = \frac{\pi}{4}(d^2 - d_i^2)$. The thin-wall form $p\,d_i/(4t)$ of AS 1210 Appendix H, H4.2 is the approximation this replaces; it over-reads the wall by a factor $(d_i + t)\,/d_i$.

General membrane longitudinal stresses (points A_u to D_L) due to pressure:

$$P_{r,m} = \frac{p\,d_i^2}{d_o^2 - d_i^2} \tag{C.30}$$

Both terms take d_i in the *corroded* condition, $d_i = d_o - 2(t - c_n)$, matching every other WRC term in this chapter and ASME BPVC.VIII.2 §4.1.4.1.

Total membrane longitudinal stresses (points A_u to B_L):

$$\sigma_{r,m} = \sigma_{r,m}(F) + \sigma_{r,m}(M_L) + \sigma_{r,p} \tag{C.31}$$

Total membrane longitudinal stresses (points C_u to D_L):

$$\sigma_{r,m} = \sigma_{r,m}(F) + \sigma_{r,m}(M_C) + \sigma_{r,p} \tag{C.32}$$

Total longitudinal stresses (points A_u to B_L):

$$\sigma_r = \sigma_{r,m}(F) + \sigma_{r,b}(F) + \sigma_{r,m}(M_L) + \sigma_{r,b}(M_L) + \sigma_{r,p} \tag{C.33}$$

Total longitudinal stresses (points C_u to D_L):

$$\sigma_r = \sigma_{r,m}(F) + \sigma_{r,b}(F) + \sigma_{r,m}(M_C) + \sigma_{r,b}(M_C) + \sigma_{r,p} \tag{C.34}$$

C.2.3 Shear stresses

Shear stresses (points A_u to D_L) from torsional moment M_t:

$$\tau(M_t) = \frac{M_t}{2\pi r_0^2 t} \tag{C.35}$$

Shear membrane stresses (points A_u to B_L) from shear force F_C:

$$\tau(F_C) = \frac{F_C}{\pi r_0 t} \tag{C.36}$$

Shear membrane stresses (points C_u to D_L) from shear force F_L:

$$\tau(F_L) = \frac{F_L}{\pi r_0 t} \tag{C.37}$$

Total shear stresses (points A_u to B_L):

$$\tau = \tau(M_t) + \tau(F_C) \tag{C.38}$$

Total shear stresses (points C_u to D_L):

$$\tau = \tau(M_t) + \tau(F_L) \tag{C.39}$$

C.2.4 Total stresses

General membrane stresses due to pressure $P_m(\theta)$ are defined above in the circumferential and longitudinal sections.

The junction is a plane-stress state ($\sigma_3 \approx 0$), so the local stresses are reduced to the combined stress intensity S of WRC 297 §3.4 — the maximum-shear (Tresca) measure of WRC 537 §1.1, §3.3.5 and Tables 2 and 3: the largest difference between the principal stresses of $(\sigma_r, \sigma_\theta, \tau)$, the third principal being zero. ASME BPVC.VIII.2 Part 5 supplies the limits S is compared against (§5.2.2.4 for P_m and S_{PL}, §5.5.6.1(d) for S_{PS}), not the combination rule. §5.2.2.1(b) would equally permit the von Mises equivalent; maximum shear is the more conservative of the two — at most $2/\sqrt{3} = 15.5\%$ higher — so the margins reported here are on the safe side.

Membrane stress (points A_u to D_L):

$$\begin{aligned} R_m &= \sqrt{\left(\sigma_{r,m} - \sigma_{\theta,m}\right)^2 + 4\,\tau^2}, \qquad p_{1,2}\Big|_m = \tfrac{1}{2}\left(\sigma_{r,m} + \sigma_{\theta,m} \pm R_m\right) \\ \sigma_m &= \max\left\{\ |p_1|\,,\ |p_2|\,,\ R_m\right\} \end{aligned} \tag{C.40}$$

where $\sigma_{\theta,m}$, $\sigma_{r,m}$ and τ are the total membrane circumferential, longitudinal and shear components at the point.

Total stress (points A_u to D_L):

$$\begin{aligned} &R = \sqrt{\left(\sigma_r - \sigma_\theta\right)^2 + 4\,\tau^2}, \qquad p_{1,2} = \tfrac{1}{2}\left(\sigma_r + \sigma_\theta \pm R\right), \qquad \sigma_{\text{eqv}} = \max\left\{\ |p_1|\,,\ |p_2|\,,\ R\right\} \\ &\sigma = \max\left\{\sigma_{\text{eqv}}\Big|_u,\ \sigma_{\text{eqv}}\Big|_l,\ \sigma_m\right\} \end{aligned} \tag{C.41}$$

where σ_θ and σ_r are the total circumferential and longitudinal stresses and τ is the total shear. The outer (u) and inner (l) fibres of a point pair are reduced together and the larger governs, so both rows of a pair carry the same σ.

C.2.5 Worked Example — Governing Point

The equations above are restated here with the values this calculation actually used. Point Au governs — it carries the largest total stress intensity of the eight junction points and is classified PL+Pb+Q. Per-term values for every point are tabulated in Table 5.1; the coefficients behind the force- and moment-driven terms are the chart reads summarised in Table B.1.

Loads at the nozzle–shell junction (as applied to the WRC read, after any off-radial transformation):

$$F = 2500.0000\ \text{N}, \quad V_C = 600.0000\ \text{N}, \quad V_L = 750.0000\ \text{N}, \tag{C.42}$$

$$M_C = 400.0000\ \text{N m}, \quad M_L = 400.0000\ \text{N m}, \quad M_t = 300.0000\ \text{N m} \tag{C.43}$$

Total membrane circumferential stress (Eq. (C.16)):

$$\begin{aligned} \sigma_{\theta,m} &= \sigma_{\theta,m}(F) + \sigma_{\theta,m}(M_L) + \sigma_{\theta p} \\ &= (-0.4899) + (-0.2635) + (158.9078) \\ &= 158.1544\ \text{MPa} \end{aligned} \tag{C.44}$$

Total circumferential stress (Eq. (C.18)). WRC 297 gives the nozzle no circumferential *bending* term (§3.1, Eqs. (7) and (8)), so the total is the membrane total above:

$$\sigma_\theta = \sigma_{\theta,m} = 158.1544\ \text{MPa} \tag{C.45}$$

Total membrane longitudinal stress (Eq. (C.31)):

$$\begin{aligned} \sigma_{r,m} &= \sigma_{r,m}(F) + \sigma_{r,m}(M_L) + \sigma_{r,p} \\ &= (-0.2044) + (-0.5348) + (5.9111) \\ &= 5.1718\ \text{MPa} \end{aligned} \tag{C.46}$$

Total longitudinal stress (Eq. (C.33)):

$$\begin{aligned} \sigma_r &= \sigma_{r,m} + \sigma_{r,b}(F) + \sigma_{r,b}(M_L) \\ &= (5.1718) + (-5.5648) + (-4.3675) \\ &= -4.7604\ \text{MPa} \end{aligned} \tag{C.47}$$

Total shear stress (Eq. (C.38)):

$$\begin{aligned} \tau &= \tau(M_t) + \tau(F_C) \\ &= (0.1697) + (0.0927) \\ &= 0.2624\ \text{MPa} \end{aligned} \tag{C.48}$$

Stress intensities — the three components above are reduced by Eq. (C.40) and Eq. (C.41):

$$\begin{aligned} &R_m = \sqrt{(\sigma_{r,m} - \sigma_{\theta,m})^2 + 4\,\tau^2}, \qquad p_{1,2}\Big|_m = \tfrac{1}{2}\,(\sigma_{r,m} + \sigma_{\theta,m} \pm R_m) \\ &R_m = \sqrt{\Big((5.1718) - (158.1544)\Big)^2 + 4\,(0.2624)^2}, \qquad p_{1,2}\Big|_m = \tfrac{1}{2}\Big((5.1718) + (158.1544) \pm R_m\Big) \\ &\sigma_m = \max\Big\{\ |p_1|\,,\ |p_2|\,,\ R_m\Big\} = 158.1549\ \text{MPa} \end{aligned} \tag{C.49}$$

$$R = \sqrt{(\sigma_r - \sigma_\theta)^2 + 4\,\tau^2}, \qquad p_{1,2} = \tfrac{1}{2}\left(\sigma_r + \sigma_\theta \pm R\right), \qquad \sigma_{\text{eqv}} = \max\left\{\ |p_1|\,,\ |p_2|\,,\ R\right\}$$
$$R = \sqrt{\Big((-4.7604) - (158.1544)\Big)^2 + 4\,(0.2624)^2}, \qquad p_{1,2} = \tfrac{1}{2}\Big((-4.7604) + (158.1544) \pm R\Big)$$
$$\sigma = \max\left\{\sigma_{\text{eqv}}\Big|_u,\ \sigma_{\text{eqv}}\Big|_l,\ \sigma_m\right\} = 162.9157\ \text{MPa} \tag{C.50}$$

The general primary membrane stress from pressure alone — the $P_{\theta,m}$ and $P_{r,m}$ of Eq. (C.15) and Eq. (C.30), as reduced by the calc engine — is

$$P_m = 92.8200\ \text{MPa} \tag{C.51}$$

These three values — σ_m, σ and P_m — are the ones compared against the allowable limits in the Results chapter.

C.3 Vessel Pressure and Example Calculation

Unless distribution multipliers are applied, the WRC 537 distribution factors are taken as unity in this example: $K_n = K_b = 1.0$ (WRC 537, Appendix C, Sections C.3.1–C.3.2).

C.3.1 Circumferential stresses, σ_θ

Circumferential membrane stresses (points A_u to B_L) due to external force F:

$$\sigma_{\theta,m}(F) = K_n\left(\frac{N_\theta}{F/R_m}\right)\frac{F}{R_m T} \tag{C.52}$$

Coefficient from Figure B.28.

Circumferential membrane stresses (points C_u to D_L) due to external force F:

$$\sigma_{\theta,m}(F) = K_n\left(\frac{N_\theta}{F/R_m}\right)\frac{F}{R_m T} \tag{C.53}$$

Coefficient from Figure B.25.

Circumferential bending stresses (points A_u to B_L) due to external force F:

$$\sigma_{\theta,b}(F) = K_b\left(\frac{M_\theta}{F}\right)\frac{6F}{T^2} \tag{C.54}$$

Coefficient from Figure B.22.

Circumferential bending stresses (points C_u to D_L) due to external force F:

$$\sigma_{\theta,b}(F) = K_b\left(\frac{M_\theta}{F}\right)\frac{6F}{T^2} \tag{C.55}$$

Coefficient from Figure B.17.

Circumferential membrane stresses (points C_u to D_L) due to M_C moment:

$$\sigma_{\theta,m}(M_C) = K_n \left(\frac{N_\theta}{M_C/(R_m^2 \beta)} \right) \frac{M_C}{R_m^2 \beta T} \tag{C.56}$$

Coefficient from Figure B.23.

Circumferential bending stresses (points C_u to D_L) due to M_C moment:

$$\sigma_{\theta,b}(M_C) = K_b \left(\frac{M_\theta}{M_C/(R_m \beta)} \right) \frac{6M_C}{R_m \beta T^2} \tag{C.57}$$

Coefficient from Figure B.13.

Circumferential membrane stresses (points A_u to B_L) due to M_L moment:

$$\sigma_{\theta,m}(M_L) = K_n \left(\frac{N_\theta}{M_L/(R_m^2 \beta)} \right) \frac{M_L}{R_m^2 \beta T} \tag{C.58}$$

Coefficient from Figure B.24.

Circumferential bending stresses (points A_u to B_L) due to M_L moment:

$$\sigma_{\theta,b}(M_L) = K_b \left(\frac{M_\theta}{M_L/(R_m \beta)} \right) \frac{6M_L}{R_m \beta T^2} \tag{C.59}$$

Coefficient from Figure B.15.

Circumferential stress (points A_u to B_L) due to internal pressure:

$$\sigma_{\theta,p} = k_{\theta,p} \frac{pD_m}{2T} \tag{C.60}$$

Per the pressure coefficient definition, see Equation (C.8).

Circumferential stress (points C_u to D_L) due to internal pressure:

$$\sigma_{\theta,p} = \frac{pD_m}{2T} \tag{C.61}$$

Per the pressure coefficient definition, see Equation (C.8).

General membrane circumferential stress (points A_u to D_L) due to pressure:

$$P_{\theta,m} = \frac{pD_m}{2T} \tag{C.62}$$

Per the pressure coefficient definition, see Equation (C.8).

Total membrane circumferential stress (points A_u to B_L):

$$\sigma_{\theta,m} = \sigma_{\theta,m}(F) + \sigma_{\theta,m}(M_L) + \sigma_{\theta,p} \tag{C.63}$$

Total membrane circumferential stress (points C_u to D_L):

$$\sigma_{\theta,m} = \sigma_{\theta,m}(F) + \sigma_{\theta,m}(M_C) + \sigma_{\theta,p} \tag{C.64}$$

Total circumferential stress (points A_u to B_L):

$$\sigma_\theta = \sigma_{\theta,m}(F) + \sigma_{\theta,b}(F) + \sigma_{\theta,m}(M_L) + \sigma_{\theta,b}(M_L) + \sigma_{\theta,p} \tag{C.65}$$

Total circumferential stress (points C_u to D_L):

$$\sigma_\theta = \sigma_{\theta,m}(F) + \sigma_{\theta,b}(F) + \sigma_{\theta,m}(M_C) + \sigma_{\theta,b}(M_C) + \sigma_{\theta,p} \tag{C.66}$$

C.3.2 Longitudinal stresses, σ_r

Longitudinal membrane stresses (points A_u to B_L) of external force F:

$$\sigma_{r,m}(F) = K_n\left(\frac{N_x}{F/R_m}\right)\frac{F}{R_m\,T} \tag{C.67}$$

Coefficient from Figure B.25.

Longitudinal membrane stresses (points C_u to D_L) of external force F:

$$\sigma_{r,m}(F) = K_n\left(\frac{N_x}{F/R_m}\right)\frac{F}{R_m\,T} \tag{C.68}$$

Coefficient from Figure B.28.

Longitudinal bending stresses (points A_u to B_L) of external force F:

$$\sigma_{r,b}(F) = K_b\left(\frac{M_x}{F}\right)\frac{6F}{T^2} \tag{C.69}$$

Coefficient from Figure B.16.

Longitudinal bending stresses (points C_u to D_L) of external force F:

$$\sigma_{r,b}(F) = K_b\left(\frac{M_x}{F}\right)\frac{6F}{T^2} \tag{C.70}$$

Coefficient from Figure B.21.

Longitudinal membrane stresses (points C_u to D_L) from M_C moment:

$$\sigma_{r,m}(MC) = K_n\left(\frac{N_x}{MC/(R_m^2\,\beta)}\right)\frac{MC}{R_m^2\,\beta\,T} \tag{C.71}$$

Coefficient from Figure B.26.

Longitudinal bending stresses of M_C moment:

$$\sigma_{r,b}(MC) = K_b\left(\frac{M_x}{MC/(R_m\,\beta)}\right)\frac{6MC}{R_m\,\beta\,T^2} \tag{C.72}$$

Coefficient from Figure B.18.

Longitudinal membrane stresses (points A_u to B_L) from M_L moment:

$$\sigma_{r,m}(ML) = K_n\left(\frac{N_x}{ML/(R_m\,\beta)}\right)\frac{ML}{R_m^2\,\beta\,T} \tag{C.73}$$

Coefficient from Figure B.27.

Longitudinal bending stresses of M_L moment:

$$\sigma_{r,b}(ML) = K_b\left(\frac{M_x}{ML/(R_m\,\beta)}\right)\frac{6ML}{R_m\,\beta\,T^2} \tag{C.74}$$

Coefficient from Figure B.20.

Longitudinal stress (points C_u to D_L) due to internal pressure:

$$\sigma_{r,p} = k_{r,p} \frac{pD_m}{4T} \tag{C.75}$$

Per the pressure coefficient definition, see Equation (C.9).

Longitudinal stress (points A_u to B_L) due to internal pressure:

$$\sigma_{r,p} = \frac{pD_m}{4T} \tag{C.76}$$

Per the pressure coefficient definition, see Equation (C.9).

General membrane longitudinal stress (points A_u to D_L) due to pressure:

$$P_{r,m} = \frac{pD_m}{4T} \tag{C.77}$$

Per the pressure coefficient definition, see Equation (C.9).

Total membrane longitudinal stresses (points A_u to B_L):

$$\sigma_{r,m} = \sigma_{mx}(F) + \sigma_{mx}(ML) + \sigma_{r,p} \tag{C.78}$$

Total membrane longitudinal stresses (points C_u to D_L):

$$\sigma_{r,m} = \sigma_{mx}(F) + \sigma_{mx}(MC) + \sigma_{r,p} \tag{C.79}$$

Total longitudinal stresses (points A_u to B_L):

$$\sigma_r = \sigma_{r,m}(F) + \sigma_{r,b}(F) + \sigma_{r,m}(ML) + \sigma_{r,b}(ML) + \sigma_{r,p} \tag{C.80}$$

Total longitudinal stresses (points C_u to D_L):

$$\sigma_r = \sigma_{r,m}(F) + \sigma_{r,b}(F) + \sigma_{r,m}(MC) + \sigma_{r,b}(MC) + \sigma_{r,p} \tag{C.81}$$

C.3.3 Shear stresses

Shear stresses (points A_u to D_L) due to torsional moment M_t:

$$\tau(M_t) = \frac{M_t}{2\,\pi\,r_0^2\,(T-c)} \tag{C.82}$$

Shear membrane stresses (points A_u to B_L) due to F_C:

$$\tau(F_C) = \frac{F_C}{\pi\,r_0\,(T-c)} \tag{C.83}$$

Shear membrane stresses (points C_u to D_L) due to F_L:

$$\tau(F_L) = \frac{F_L}{\pi\,r_0\,(T-c)} \tag{C.84}$$

Total shear stresses (points A_u to B_L):

$$\tau = \tau(M_t) + \tau(F_C) \tag{C.85}$$

Total shear stresses (points C_u to D_L):

$$\tau = \tau(M_t) + \tau(F_L) \tag{C.86}$$

C.3.4 Total stresses

The junction is a plane-stress state ($\sigma_3 \approx 0$), so the local stresses are reduced to the WRC 537 combined stress intensity S — the maximum-shear (Tresca) measure of WRC 537 §1.1, §3.3.5 and Tables 2 and 3: the largest difference between the principal stresses of $(\sigma_r, \sigma_\theta, \tau)$, the third principal being zero. ASME BPVC.VIII.2 Part 5 supplies the limits S is compared against (§5.2.2.4 for P_m and S_{PL}, §5.5.6.1(d) for S_{PS}), not the combination rule. §5.2.2.1(b) would equally permit the von Mises equivalent; maximum shear is the more conservative of the two — at most $2/\sqrt{3} = 15.5\%$ higher — so the margins reported here are on the safe side.

Membrane stress (points A_u to D_L):

$$
\begin{aligned}
&R_m = \sqrt{\left(\sigma_{r,m} - \sigma_{\theta,m}\right)^2 + 4\,\tau^2}, \qquad p_{1,2}\Big|_m = \tfrac{1}{2}\left(\sigma_{r,m} + \sigma_{\theta,m} \pm R_m\right) \\
&\sigma_m = \max\left\{\ |p_1|\,,\ |p_2|\,,\ R_m\right\}
\end{aligned}
\tag{C.87}
$$

where $\sigma_{\theta,m}$, $\sigma_{r,m}$ and τ are the total membrane circumferential, longitudinal and shear components at the point.

Total stress (points A_u to D_L):

$$
\begin{aligned}
&R = \sqrt{\left(\sigma_r - \sigma_\theta\right)^2 + 4\,\tau^2}, \qquad p_{1,2} = \tfrac{1}{2}\left(\sigma_r + \sigma_\theta \pm R\right), \qquad \sigma_{\text{eqv}} = \max\left\{\ |p_1|\,,\ |p_2|\,,\ R\right\} \\
&\sigma = \max\left\{\ \sigma_{\text{eqv}}\Big|_u,\ \sigma_{\text{eqv}}\Big|_l,\ \sigma_m\right\}
\end{aligned}
\tag{C.88}
$$

where σ_θ and σ_r are the total circumferential and longitudinal stresses and τ is the total shear. The outer (u) and inner (l) fibres of a point pair are reduced together and the larger governs, so both rows of a pair carry the same σ.